

Final Degree Project

Correlation between ageing-related morphological and functional cardiac changes, the degree of cerebral atrophy, and the appearance of white matter hyperintensities

Magnetic Resonance Imaging study within a population-based cohort

Author: **Francesc Tarrús Escalada**

Clinical tutor: Víctor Pineda Sánchez

Methodological tutor: David Gallardo Giralt

Girona, November 2023

I extend my heartfelt appreciation to Dr. Víctor Pineda, my insightful tutor, for suggesting this project and for the trust. His guidance and support have been instrumental in the successful completion of this assignment.

A big thank you to my methodological tutor, Dr. David Gallardo, for mentoring me through the methodological aspects and addressing any doubts I had throughout my project.

To the entire team that is part of The Aging Imageomics study, especially to Dr. Josep Puig and Carles Biarnés. Their assistance and knowledge have made this work possible. Thank you very much for allowing me to be part of this great project, which has only just begun.

I would like to express my special thanks to Dr. Rafael Ramos and Lluís Zacarías for their dedication, their help with the statistical analysis, and the hours spent with us making sure we understood everything.

I would also like to make a special mention to the patients and their families who, completely selflessly, have allowed the realization of this project. With their invaluable collaboration, they have contributed their efforts, which in the not-too-distant future will bear fruit in helping to improve the health of individuals.

Finally, I want to express my gratitude to my family and friends for the comforting hugs and unwavering support they provided throughout this entire period. And to Georgina, for always being there.

INDEX

1. ABSTRACT	5
2. ABBREVIATIONS	6
3. INTRODUCTION	8
3.1. DEFINITION OF AGEING	8
3.2. EPIDEMIOLOGY	8
3.2.1. Worldwide epidemiology of ageing.....	8
3.2.2. Spanish epidemiology and demographic of ageing.....	8
3.3. BIOLOGICAL AGE	9
3.4. ETIOPATHOGENESIS	10
3.4.1. Molecular level.....	11
3.4.2. Cellular level	12
3.4.3. Systemic level	13
3.5. THE AGING IMAGEOMICS STUDY	13
3.6. NEUROLOGICAL AGEING	14
3.6.1. Brain – heart axis	16
3.7. CARDIAC AGEING	17
3.8. CAROTID ARTERY STENOSIS	20
3.9. MAGNETIC RESSONANCE IMAGING	21
3.9.1. Artificial Intelligence in MRI studies	21
4. JUSTIFICATION	23
5. HYPOTHESES	25
5.1. MAIN HYPOTHESES	25
5.2. SECONDARY HYPOTHESES	25
6. OBJECTIVES	26
6.1. MAIN OBJECTIVES	26
6.2. SECONDARY OBJECTIVES	26
7. MATERIAL AND METHODS	27
7.1. STUDY DESIGN	27
7.2. STUDY POPULATION AND SAMPLING	27
7.2.1. Inclusion criteria	28

7.2.2.	Exclusion criteria	28
7.3.	STUDY PROCEDURES.....	29
7.4.	WHOLE-BODY MRI ACQUISITION PROTOCOL	29
7.5.	CAROTID ULTRASOUND STUDY	31
7.6.	VARIABLES.....	32
7.6.1.	Main variables	32
7.6.2.	Secondary variables.....	33
7.6.3.	Covariates.....	33
7.7.	DATA HANDLING AND STORAGE.....	34
7.8.	FIELDWORK	34
7.9.	STATISTICAL ANALYSIS.....	36
7.10.	ETHICAL CONSIDERATIONS	37
8.	RESULTS.....	39
8.1.	BIVARIATE ANALYSIS	43
8.2.	MULTIVARIATE ANALYSIS	45
9.	DISCUSSION	48
10.	STUDY LIMITATIONS.....	50
11.	CONCLUSIONS.....	51
12.	BIBLIOGRAPHY.....	52
13.	ANNEXES	58
13.1.	ANNEX 1 – ETHICS COMMITTEE PROJECT APPROVAL.....	58
13.2.	ANNEX 2 – INFORMATION SHEET FOR PARTICIPANTS	59
13.3.	ANNEX 3 – INFORMED CONSENT	65
13.4.	ANNEX 4 – REFUSE TO BE INFORMED OF INCIDENTAL FINDINGS	66
13.5.	ANNEX 5 – ANALYSIS ADJUSTED FOR AGE.....	67
13.6.	ANNEX 6 – ANALYSIS ADJUSTED FOR DEGREE OF STENOSIS	68

1. ABSTRACT

INTRODUCTION. Ageing is a multisystemic process that makes individuals more susceptible to diseases and functional limitations. Life expectancy has increased, which implies that by 2030, one in six people will be 60 or older, reflecting global trends as seen in Spain. This study focuses on the link between heart and brain ageing, inspired by The Aging Imageomics Study. The main objective is assessing the relation between the left ventricle's (LV) morphological changes with white matter hyperintensities (WMH) and cerebral atrophy.

METHODS. This project is an observational prospective study that analyzes data from The Aging Imageomics population study in the province of Girona. It investigates the heart-brain ageing relationship using a portable 1.5 Tesla MRI scanner with data from 1,030 participants aged 50 or older, coming from the MESGI50 and MARK studies. Cardiac images were obtained via electrocardiographic synchronization, while cerebral images were acquired using T2-weighted sequence (MP RAGE). Statistical analysis was conducted with R software, including descriptive analysis with T-student and Welch's t-tests, as well as bivariate and multivariate analysis using linear regression models.

RESULTS. The study included 1,030 participants. The average age was 66.81 years with nearly-equal gender distribution. In the multivariate analysis, statistical significance in findings diminished when adjusting for age, sex, and carotid stenosis. An increase of 1 gram in LV mass corresponds to a 0.04ml increase in WMH volume ($p = 0.004$). Furthermore, right ventricle's (RV) end-diastolic volume is positively correlated with total grey volume ($p = 0.042$), while RV end-systolic volume is linked to increases in total grey volume and cortex volume ($p = 0.027$ and $p = 0.022$, respectively).

CONCLUSION. This study shows a strong relationship between LV mass and WMH. While functional and morphological left ventricle variables have no effect on cerebral atrophy. The study did not find a link between functional ventricle changes and WMH. The research hints at a potential correlation between RV volumes and increased total grey matter, opening up avenues for future investigations.

2. ABBREVIATIONS

- **A'**: Left ventricle active filling during late diastole
- **AD**: Alzheimer's disease
- **AFib**: Atrial fibrillation
- **AI**: Artificial intelligence
- **BBB**: Blood-brain barrier
- **CEIC**: Clinical Research Ethics Committee
- **CI**: Confidence interval
- **DNA**: Deoxyribonucleic acid
- **E'**: Left ventricle passive filling during early diastole
- **ECM**: Extracellular matrix
- **g**: Gram
- **GBA**: Gut-brain axis
- **GCS**: Global circumferential strain
- **GH**: Growth hormone
- **GLS**: Global longitudinal strain
- **IDIBGI**: Institut d'Investigació Biomèdica de Girona
- **IGF-1**: Insulin-like growth factor
- **INE**: Instituto Nacional de Estadística
- **l**: Litres
- **LA**: Left atrium
- **LV**: Left ventricle
- **LVEF**: Left ventricle ejection fraction
- **m²**: Square meter
- **MARK**: Improving interMediAte RisK management study
- **MESA**: Multi-Ethnic Study of Atherosclerosis
- **MESGI50**: Maturity and Satisfactory Ageing in Girona study
- **ml**: Millilitre
- **MP RAGE**: Magnetization-prepared rapid acquisition gradient echo

- **MRI:** Magnetic Resonance Imaging
- **PD:** Parkinson's disease
- **RNA:** Ribonucleic acid
- **ROS:** Reactive oxygen species
- **RV:** Right ventricle
- **SARS-CoV-2:** Severe Acute Respiratory Syndrome Coronavirus 2
- **SASP:** Senescence-associated secretory phenotype
- **SD:** Standard deviation
- **SHARE:** Survey of Health, Aging, and Retirement in Europe.
- **SSFP:** Steady-state free precession
- **WMH:** White matter hyperintensities

3. INTRODUCTION

3.1. DEFINITION OF AGEING

Ageing is a ubiquitous biological process characterized by an increasing vulnerability to pathology, loss of adaptive response to life challenges and functional limitations (1). This progressive and irreversible decline affects most if not all tissues and organs of the body, and it is well known as an independent risk factor in many major diseases; such as cardiovascular, neurodegenerative disorders and cancer (2).

3.2. EPIDEMIOLOGY

3.2.1. *Worldwide epidemiology of ageing*

According to the World Health Organization, the proportion of elderly people is increasing at an unprecedented pace. It is expected that by 2030 1 in 6 people in the world will be aged 60 years or over. Whereas, the number of people aged 80 years or older, it is foreseen to triple between 2020 and 2050 (3). With the establishment and improvement of the public health system, human life expectancy has increased significantly from around 50 years in the early 1900s to over 80 at the present time (4). Therefore, it would imply an escalation in the number of ageing-related diseases, establishing fundamental changes to the population structure, and having a profound influence on individuals' lives and society at large (5,6).

3.2.2. *Spanish epidemiology and demographic of ageing*

Considering Spain, our nation's epidemiology is not different from the trend in the rest of the world, posing a major social and economic challenge for the main developed economies. As of January 1st 2021, 19.65% of the total population were older people¹, and the average age of the population now is 43.81 years when in 1970 it was 32.7. Despite the decline of 1.25 years compared to 2019, attributed to the exceptional circumstances arising from the SARS-CoV-2 pandemic, life expectancy has experienced a remarkable increase throughout the 20th century. The current trend indicates that it will

¹ An older person is defined by the United Nations as an individual who is over 60 years of age (7).

continue to do so. As per the most recent mortality statistics from Instituto Nacional de Estadística (INE), women in Spain have a life expectancy at birth of 85.06 years, whereas men have a life expectancy of 79.59 years; both of them are among the highest in the European Union. Life expectancy lengthening has been a result of the decrease in infant mortality, which is a reflection of the historical progress in health, social and economic conditions, and the improvement in lifestyles.

If we look at territorial ageing, Asturias, Galicia, and Castilla y León are the autonomous communities with the highest average age in Spain, as they all exceed 20% of elderly people out of their total population.

Between 1958 and 1977, the *baby boom* generation was born. As we come closer to 2024, this generation will begin their retirement. This, combined with the decline in birth rates, will result in an increased burden on social protection systems, which will compromise citizens pensions and public health systems (8).

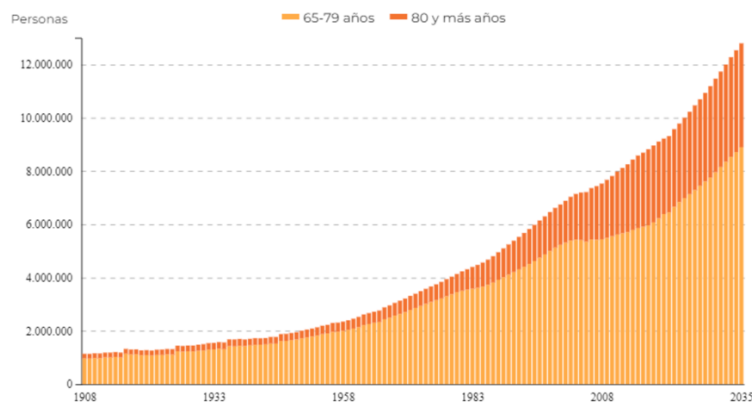


Figure 1 - Population aged 65 and over. Spain, 1908-2035.

In light orange we can observe the population aged between 65-79 years. And, in dark orange the ones aged 80 years or older. *Source: Human Mortality Database. Life tables with data between 1908 and 2019; INE and Estadísticas del Padrón Continuo (2020-2021) (8).*

3.3. BIOLOGICAL AGE

Age signifies several presumptions as to the biological state, fitness and functioning of the person in question. It also structures our social existence and binds us to society (9). It is typically expressed as chronological age, which is measured as years since birth. But clinicians have found that this so-called chronological age is not an adequate estimate of the ageing process because of the heterogeneity in the health outcomes, especially in

older individuals (10). That is why, in recent years, the concept of biological age has emerged not only considering the time elapsed, but also correlating nutrition, lifestyle, genetics and comorbidities. Although it is not easily evaluated due to the lack of consensus on its determination, it aims to give a better calculation of the ageing process (11).

Healthy ageing is a perfect balance of biological and chronological senescence. This is exceptionally complex to determine since there is no evidence of widespread ageing physiopathology throughout the different body systems. Actually, The Aging Imageomics Study was created as a common ground for its study [See section 3.5. “The Aging Imageomics study”].

3.4. ETIOPATHOGENESIS

Research on the mechanisms of ageing is a very active area. For thousands of years, a healthy longevity has been the goal pursued by human beings. New achievements made in this ongoing investigation have managed to classify three different categories: molecular level, cellular level and systematic alterations (6). This information broads a better understanding of the multiple signalling networks involved in the ageing process of organisms.

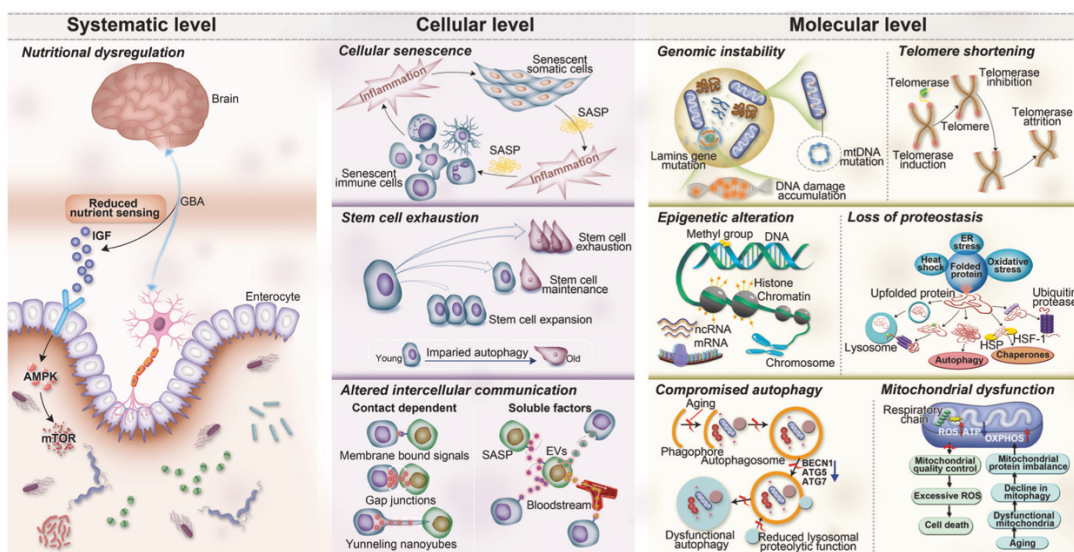


Figure 2 - The ten hallmarks of ageing subdivided into three categories

Molecular hallmarks (genomic instability, telomere dysfunction, epigenetic alterations, loss of proteostasis, compromise of autophagy, and mitochondrial dysfunction), cellular hallmarks (cellular senescence, stem cell exhaustion, and altered intercellular communication), and systemic alterations (deregulated nutrient sensing).

Abbreviations: AMPK: Protein kinase AMP-activated catalytic subunit alpha 1, ATG5: Autophagy-related 5, ATG7: Autophagy-related 7, ATP: Adenosine triphosphate, BECN1: Beclin 1, ER: Endoplasmic reticulum stress, EVs: Extracellular vesicles, GBA: Gut–brain axis, HSF-1: Heat shock factor-1, HSP: Heat shock protein, IGF: Insulin-like growth factor-1, mtDNA: Mitochondrial DNA, mRNA: Messenger RNA, mTOR: Mechanistic target of rapamycin kinase, ncRNA: Noncoding RNA, OXPHOS: Oxidative phosphorylation, Rb: Retinoblastoma, ROS: Reactive oxygen species, SASP: Senescence-associated secretory phenotype.

Source: *Aging and aging-related diseases: from molecular mechanisms to interventions and treatments* (6).

3.4.1. Molecular level

Corresponding to the molecular level, genomic instability is an important cause of cellular senescence in many species and has an important role in tumorigenesis. The sporadic replication or repair errors that lead to gene expression deregulation are primarily responsible for this phenomenon, but it can also occur in response to developmental or environmental signals (12).

With each successive cell division, telomeric deoxyribonucleic acid (DNA) undergoes progressive shortening. When this shortening reaches a critical level known as the Hayflick limit², it triggers dysfunction within the telomeres, eliciting a DNA damage response. Consequently, this instigates cell cycle arrest and the upregulation of proinflammatory factors, culminating in the process of organismal ageing (14).

Epigenetics encompasses the processes of activating or repressing genes without introducing changes to the DNA sequence itself. Mechanisms include a range of processes, such as DNA methylation, modifications to histones, remodelling of chromatin structure, and transcriptional modifications facilitated by noncoding RNAs (6).

When proteins lose their capacity to undergo efficient folding and assembly, the resultant toxic aggregation arising from the loss of proteostasis can induce cellular dysfunction. Thus ultimately culminating in cell death and the appearance of aggregate-deposition diseases, just as alpha-synuclein in Parkinson's disease (PD) and amyloid-beta and Tau in Alzheimer's disease (AD) (15).

² The Hayflick limit consists on the number of times a normal cell population divides before entering the senescence phase (13).

Autophagy is a highly conserved pathway that degrades cellular components, like defective organelles and aggregates of misfolded protein through lysosomes. Evidence suggests that autophagic activity decreases with age, promoting the development of age-related diseases (16).

The average quality of the mitochondria in each cell worsens as individuals transcend into elderly stages of their life. The mitochondrial activity degeneration results in a redox imbalance and an increased abundance of reactive oxygen species (ROS). This, coupled with the impaired mitophagy (degradation of the mitochondria by autophagy), leads to an increased metabolic stress (17).

3.4.2. Cellular level

The cellular level tries to understand the structure, function, and properties of cells. In this group, we find cellular senescence to be an important contributor. It can be defined as a state of irreversible proliferative termination, entailing permanent cell cycle arrest. This process is regulated by broadly known tumour suppressor genes, some of which are p53, p21, p16 and p19. Senescence can be replicative, when the cell reaches its maximum number of divisions, or stress-induced, in response to DNA damage and oxidative stress (18).

One of the most conspicuous features of ageing is the diminishment of the tissues' regenerative capacity, a function for which stem cells are responsible. Multiple types of age-related damage, just like impaired autophagy, accumulation of DNA damage, or overexpression of cell cycle-inhibitory proteins, lead to stem cell exhaustion (19).

Senescent cells communicate with each other in a very complex process via soluble factors, growth factors, and extracellular matrix remodelling enzymes; all of them constituting the senescence-associated secretory phenotype (SASP). This highly secretion activity has both beneficial and detrimental effects on the neighbouring cells, depending on the activated triggers. The alteration of the intercellular communication produced via SASP affects many homeostatic processes such as proliferation or

apoptosis, this explains why investigators are developing senomorphic drugs that would inhibit the deleterious effects of the SASP (20).

3.4.3. Systemic level

Energy substrates, in particular glucose, fatty acids, and ketones are sensed through the somatotrophic axis. The aforementioned neuroendocrine pathway is specially controlled by the Growth Hormone (GH) and the Insulin-like growth factor (IGF-1). The nutrient sensing pathway's deregulation can cause the onset of diabetes, influence cancer development and favour the process of ageing by exposing cells to nutrient abundance.

Another important actor is the gut–brain axis (GBA) which, through the microbiota, weakens the blood–brain barrier (BBB) and induces neuroinflammation and ultimately, neurodegeneration (21).

Significantly, it is imperative to acknowledge that external factors including suboptimal nutrition, a sedentary way of life, psychological and social stress, smoking, and exposure to pollution, may potentially contribute to the onset of diseases by influencing on these hallmarks at various levels (22).

The course of ageing is variable and complex, partly because these processes are interconnected. Therefore, such defects in one process can have a direct or indirect repercussion in other pathways (19). The understanding of baseline molecular changes is key to correlate structural and functional damage to the main organs of our body, specially the brain and the heart.

3.5. THE AGING IMAGEOMICS STUDY

Over the last few years, it has been notorious that health promotion and primary prevention are the most effective strategies to reduce morbimortality; as well as delaying the appearance of chronic diseases associated with aging that affect our society. Initiated in the year 2000, the Multi-Ethnic Study of Atherosclerosis (MESA) in the United States, is a prospective study involving a large sample of 6,500 participants. One of its key objectives is to identify subclinical atherosclerotic markers that can anticipate the

onset of cardiovascular events, with the ultimate aim of transitioning to a personalized, disease-centric risk prediction approach (23).

The Aging Imageomics Study serves as the Spanish equivalent of the MESA study. It is a population-based observational study designed to provide more information in this area. Investigators studied a number of 1,030 participants from the province of Girona, Spain aged 50 years or older. The main objectives were to create a large bank of images obtained via Magnetic Resonance Imaging (MRI), to make an atlas of ageing of the human body, and to determine new imaging biomarkers that could predict the onset of diseases.

Participants were chosen from two ongoing studies, the Maturity and Satisfactory Ageing in Girona study (MESGI50) and the Improving interMediAte Risk management study (MARK). Partakers were all scheduled for two appointments in which they underwent a series of imaging tests, including a full-body MRI and a carotid ultrasound; also, they obtained a series of urine, stool and blood samples. At last, participants were submitted to a clinical interview, anthropometric examination, cardiovascular examination; and the completion of standardized tests to measure cognitive, mood and personality-related variables.

After acquiring all the data, the investigators possessed sufficient statistical power to make dependable assessments of correlations between imaging phenotype measures and a diverse range of parameters pertaining to ageing. The future analysis will enable us to identify age-related changes in the body, which are also known as biomarkers of ageing. The combination of these biomarkers could provide a measure of biological age and predict the onset of age-related diseases and/or residual lifetime with greater accuracy than chronological age (24).

3.6. NEUROLOGICAL AGEING

As in all dimensions of human physiology, the nervous system undergoes modifications with age. Even in the most robust elderly individuals, there is an increase in neuronal loss, heightened vascular pathology, and numerous cellular-level changes compared to healthy younger adults (25).

Despite the etiopathogenesis has already been explained [See section 3.4. "Etiopathogenesis"], we shall remind that epigenetic factors, coupled with diminished DNA repair capabilities, result in heightened cellular oxidative stress and elevated inflammatory responses. These mechanisms instigate neurodegeneration associated with ageing and contribute to the onset of neuronal senescence (6).

The ageing process is marked by a gradual reduction in brain volume, occurring at an approximate rate of 5% per decade after reaching the age of 40 (26). These leads to an atrophy of the brain, as a result of multiple morphological changes that we will now discuss.

Due to neuronal death and synapse loss, the grey matter, primarily located in the cortex and basal ganglia, undergoes a thinning process. This reduction is specific to certain regions, predominantly impacting the temporal and frontal lobes. Within the temporal lobe, the hippocampus is situated, and its atrophy contributes to cognitive decline. Research indicates that frontal volume atrophy is more prevalent in normal ageing, expressed as behavioural and personality changes, while temporal regions exhibit higher atrophy rates in AD (26).

White matter axons encased in myelin are frequently affected by an impaired blood supply and/or dysfunction of the blood–brain barrier, attributed to cardiovascular risk factors such as diabetes mellitus, smoking or high blood pressure. The deterioration of the myelin sheath surrounding these axons leads to a modification in the tissue's relaxation time, culminating in a hyperintense signal in the MRI machine. The presence of white matter hyperintensities (WMH) within the general population varies, with prevalence rates ranging from 11% to 21% in adults around the age of 64, increasing to 94% by the age of 82 (27). These hyperintensities extend from the ventricles towards the juxtacortical union and are associated with cognitive decline, neurovascular disease, and dementia (28).

Vascular modifications, manifested by the presence of microhaemorrhages, contribute to the ageing brain. Lobar microhaemorrhages, stemming from the accumulation of

amyloid plaques, and subcortical microhaemorrhages associated with hypertension, heighten the risk of vascular dementia (29).

Due to cerebral atrophy, ventricles filled with cerebrospinal fluid expand as a compensatory mechanism to uphold the brain's structure and support. Additionally, sulci widen due to volume loss (30). MRI has become a crucial tool for characterizing these morphological changes (31). It surpasses computed tomography in sensitivity for detecting sulcal changes, offering superior tissue contrast, multiplanar imaging capabilities, absence of bone artifacts, and no ionizing radiation (32).

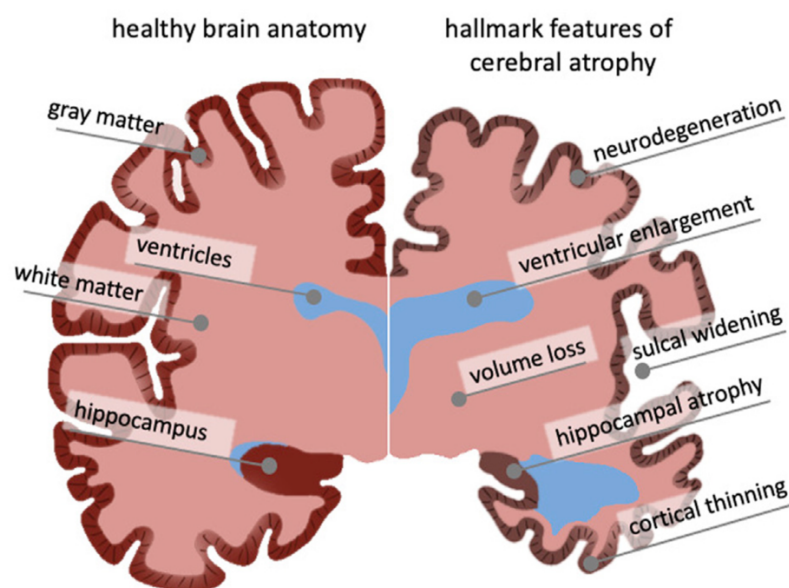


Figure 3 - Changes in the ageing brain.

Cerebral atrophy characterizes morphological changes in the ageing brain, observed in both healthy and pathological ageing. These changes encompass neurodegeneration, cortical thinning, volume loss, white matter degeneration, sulcal widening, and ventricular enlargement. Over time, subcellular and cellular aging mechanisms contribute to these organ-level changes, becoming evident in cross-sectional imaging studies. *Source: Brain Shape Changes Associated With Cerebral Atrophy in Healthy Aging and Alzheimer's Disease (30).*

3.6.1. Brain – heart axis

The relationship between cardiovascular and brain health is complex, with cardiovascular risk factors like smoking, diabetes mellitus, obesity, and hypertension appearing to play a role in the aetiopathogenesis. Notably, prior studies, including The Framingham Heart Study and the Multi-Ethnic Study of Atherosclerosis have established a correlation between these cardiovascular risk factors and conditions such as brain

atrophy, white matter hyperintensities, and cognitive decline (33,34). Moreover, research findings suggest that an increase in left ventricular mass is correlated with lower cognitive performance and an elevated risk of dementia (35,36). However, there is a lack of substantial studies that compare morphological and functional cardiac changes associated with physiological ageing, in association with the extent of cerebral atrophy and the occurrence of white matter hyperintensities.

3.7. CARDIAC AGEING

In Spain, 26% of deaths in 2022 were due to diseases of the cardiocirculatory system, being the first cause of female mortality and the second among men (37). Old age is one of the dominant risk factors for the development of these diseases. Consequentially, the need for studying the effects of cardiac ageing has become an important field of study, in order to understand and identify the pathology.

The cardiovascular system comprises various discrete cell types, encompassing endothelial cells, smooth muscle cells, cardiomyocytes, fibroblasts, and immune cells. These cells collectively collaborate to ensure the adequate circulation of blood, facilitating nutrient supply and waste removal for every cell within the organism. Operating under perpetual mechanical and metabolic stress, this intricate system experiences a cumulative escalation in the likelihood of dysfunction across molecular, cellular, and organ-wide dimensions as age advances (38).

Although the molecular mechanisms that explain ageing in cells have already been exposed [*See section 3.4. "Etiopathogenesis"*], we shall remind the ones that are more involved in the decline of the heart's function. Oxidative stress due to mitochondrial dysfunction and impaired mitophagy, deposition of misfolded proteins and the altered ECM remodelling justify the morphological changes of the heart (39).

The myocardium remodels over time, leading to a reduction in the number of cardiomyocytes as a consequence of apoptosis; those that remain suffer hypertrophy as a compensatory mechanism. If we add this to the thickening of the systemic vessels wall due to collagen deposition, it gives rise to left ventricle hypertrophy. The thickening of

the ventricular wall causes a diminishment in the size of the cardiac chambers, thus affecting specially the diastolic ventricular volume³. Also, the reduction of LV cavities and the increased LV mass due to hypertrophy, rise of the mass/volume ratio⁴ (42).

Normal diastolic filling has two phases: an early passive filling ('E') and an active filling during late diastole by atrial contraction ('A'). The slowing of myocardial relaxation and diminished compliance, caused by the LV hypertrophy, changes the rate of passive filling. As a result, the bulk of ventricular filling shifts to the active filling phase, decreasing the E/A ratio (43).

The reduction of the left ventricle chamber calls forth the left atrium to work harder during the atrial contraction phase of diastole, and it also enlarges to accommodate more volume. Diastolic dysfunction is a major problem specially for patients who suffer from atrial fibrillation (AFib), as they have an irregular heart rhythm that does not allow the atria to contract efficiently; hence, compromising the capability of augmenting late LV filling during diastole. Also, the remodelling changes that occur due to the increased volume of the atria, can induce the appearance of AFib itself (42,43).

Although the right atrium and ventricle have not been so thoroughly studied, a depletion of the right ventricle volume without changes in the right atrium have been demonstrated (44). The enlargement of the right atrium, if existent, may be secondary to tricuspid valve regurgitation; as heart valves thicken and calcify physiologically (42).

Despite the controversy, left ventricle ejection fraction (LVEF) is preserved when resting, but it is blunted during aerobic exercise. This can be explained by the diminished myocardial contractility, attenuated arterial vasodilator capacity resulting in heightened cardiac afterload⁵, and decreased responsiveness to beta-adrenergic stimulation manifest with the ageing process (39). LVEF is the most commonly used measure of

³ The diastole can be defined as the dilatation of the ventricles of the heart that follows each contraction, during which they refill with blood (40).

⁴ This ratio provides a quantitative assessment of the correlation between the weight of the left ventricle (LV mass) and its end-diastolic volume. It is employed to evaluate alterations in cardiac morphology and function (41).

⁵ The afterload is the amount of force the ventricle has to make in order to eject blood.

systolic function, but newer techniques such as the strain allow the detection of subclinical LV dysfunction before a reduction occurs in LVEF.

The strain assesses myocardial deformation. We need to take into account that our heart during systole (the moment where it pumps the blood to our vessels) performs three movements in order to contract efficiently. There is a longitudinal shortening in which the base approaches the apex, a circumferential constraint, and torsion. When the isovolumetric stage of the systole initiates, both the apex and the base rotate in a clockwise direction. During the systole, the base changes direction and starts to rotate counter clockwise, causing the torsional peak. When the isovolumetric relaxation stage initiates, the muscle fibres untwist contributing to the early passive filling phase of the diastole (45). MRI/Doppler echocardiography assessed strain objectifies the cardiac shortening, lengthening, thickening and rotation providing high sensitive estimation of the myocardial deformation (46). This parameter aids in differentiating active from passive segment movements, evaluating ventricular desynchrony and global/segmental myocardial function (47).

Research shows that with ageing, there is a lower global longitudinal strain (GLS), but a higher global circumferential strain (GCS) and higher indices of torsion. Proposing that the augmentation of torsion and GCS serves as a compensatory mechanism for the age-related reduction in GLS, consequently preserving left ventricular ejection fraction (LVEF) with the progression of age (42).

The left atrium (LA) has also been measured with strain techniques, showing that increased age is associated with lower reservoir and conduit strain (trans-mitral flow) as a result of the stiffening of the LA walls. Yet, it has an enhanced booster strain (late diastolic atrial contraction) (42).

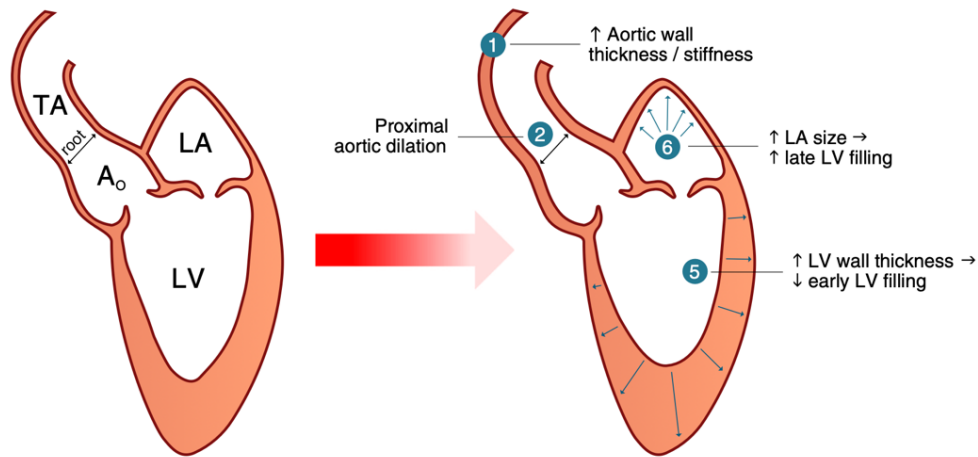


Figure 4 - Age-related changes in cardiovascular structure and function.

Abbreviations: DBP: Diastolic blood pressure, EDV: End-diastolic volume, LA: Left atrium, LV: Left ventricle, LVEF: Left ventricular ejection fraction, PP: Pulse pressure, SBP: Systolic blood pressure. *Source: Cardiac changes associated with vascular aging (39).*

3.8. CAROTID ARTERY STENOSIS

Carotid artery stenosis is a consequence of systemic atherosclerotic disease. Risk factors such as smoking, hyperlipidaemia, age, high blood pressure, and diabetes contribute to the formation of atherosclerosis deposits, primarily composed of cholesterol and fatty acids. Given that these arteries transport blood to the brain, the accumulation of sufficient material to obstruct the majority of the vessel can lead to symptoms like dizziness, fainting, and blurred vision. Another potential clinical presentation involves the occurrence of a stroke or transient ischemic attack, often secondary to the sudden formation of a blood clot (48).

We decided to include the measurement of stenosis degree using carotid ultrasound as a confounding variable in our study. This decision aims to prevent any bias that may arise from this factor.

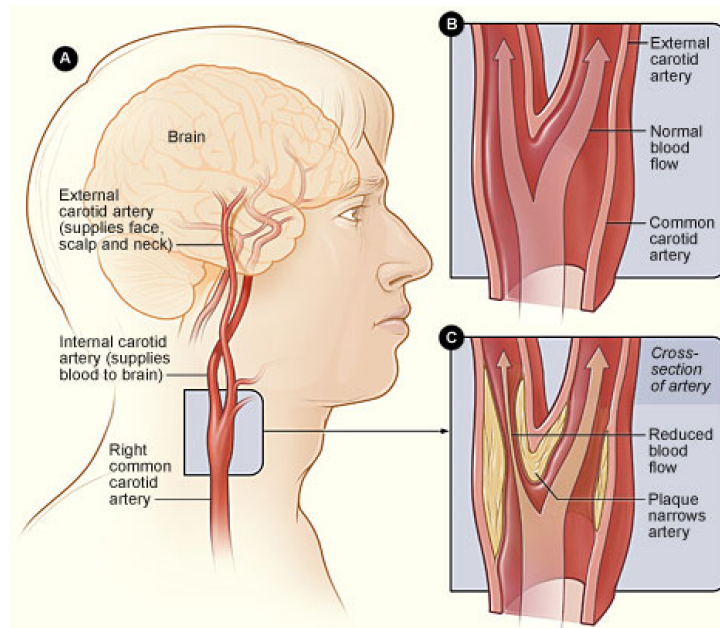


Figure 5 – Contrasts between a normal carotid artery and an occluded one.

Figure A shows the location of the right carotid artery in the head and neck. Figure B shows the inside of a normal carotid artery that has normal blood flow. Figure C shows the inside of a carotid artery that has plaque build-up and reduced blood flow. *Source: University of California San Francisco (49).*

3.9. MAGNETIC RESSONANCE IMAGING

MRI imaging has made its way into population-based studies, given that it permits a non-ionizing, non-invasive, reproducible and precise distinguishment of the organs and tissues of the human body, without the need to administer a contrast agent (50). The MRI scanner has a strong magnetic field that aligns the hydrogen nuclei's (protons) of our body normally found randomly distributed. Then a radiofrequency wave is applied, causing them to absorb energy and resonate. After turning off the radiofrequency source, protons revert to their resting state, leading to the emission of a signal. This signal is then detected by the coils and undergoes processing to generate the imaging (51). The quality of this imaging technique allows to study morphological and functional processes, being able to identify subtle changes at an early stage that might go unnoticed using alternative modalities (24).

3.9.1. Artificial Intelligence in MRI studies

Artificial intelligence (AI) has recently emerged as a widely discussed subject. Nonetheless, this science was officially born in 1956 at the Dartmouth College

conference, and defined by John McCarthy as “the science and engineering of making intelligent machines” (52). While not a novel concept, there has been remarkable advancement in the field of medicine in recent years. The significant progress can be attributed to increased computing power, digital transformation, and enhanced accessibility to data.

The application of AI in medicine enhances various aspects, including its ability to analyse vast amounts of data through *Machine learning* tools. This involves the use of mathematical algorithms that learn through experience. These innovations collectively contribute to progress, notably in elevating image quality and achieving more precise and accurate automatic analysis. Despite the considerable benefits that AI brings to the medical field, ethical, legal, and privacy considerations require careful attention (52).

As detailed in section 7.8 “*Fieldwork*”, in our study, the use of AI has improved the efficiency of the cardiac and brain MRI segmentation.

4. JUSTIFICATION

The ageing process is an inevitable phenomenon that eventually impacts all organs and tissues in our body. It is marked by an increasing vulnerability to pathology, diminished adaptive responses to life challenges, and functional limitations (1). With advancements in public health systems, human life expectancy has experienced a substantial growth from approximately 50 years in the early 1900s to over 80 at present (4).

As per the projections of the World Health Organization, it is anticipated that by 2030, 1 in 6 individuals will be aged 60 years or older (3). The epidemiological situation in Spain aligns with global trends, with 19.65% of the total population being 60 years or older as of 2021, and certain autonomous communities surpassing this percentage. This leads to an inversion of the population pyramid, attributed to declining birth rates and a significant proportion of elderly individuals (8).

Exploring the molecular, cellular, and systemic mechanisms underlying ageing is a highly intricate field. Understanding these mechanisms offers valuable insights into the ageing process and has the potential for primary prevention and treatment of diseases (6). Ageing is established as an independent risk factor in various major conditions, including cardiovascular, neurodegenerative, and cancer (2). Transitioning to prevention in an ageing population is vital. As the incidence of age-related diseases increases, it imposes an additional burden on health and social systems (8).

Similar to other aspects of human physiology, the nervous system undergoes structural and functional alterations with ageing. The decrease in brain volume, the emergence of white matter hyperintensities, protein deposition, and vascular changes contribute to the ageing brain (26,27). These changes are associated with cognitive decline, neurovascular diseases, and dementia (28).

Age-related changes in the heart primarily involve alterations in the myocardium. The remodelling of the muscle wall, resulting from apoptosis, triggers a compensatory hypertrophic mechanism. This results in an augmentation of ventricular mass and a

reduction in cardiac chamber volumes, particularly during diastole, ultimately affecting the mass/volume ratio of the left ventricle (42).

Previous investigations, including The Framingham Heart Study and The Multi-Ethnic Study of Atherosclerosis (MESA), have identified a connection between cardiovascular risk factors (i.e. smoke, obesity, hypertension and diabetes) and outcomes such as a decrease in total brain volume, the presence of white matter hyperintensities, and cognitive decline (33,34). However, there has been limited discourse on the correlation between morphological and functional cardiac changes linked to physiological ageing and the degree of cerebral atrophy and the occurrence of white matter hyperintensities.

Our research derives its foundation from The Aging Imageomics Study. Serving as the Spanish counterpart of the MESA study, it is a population-based observational study involving 1,030 participants aged 50 years or older from the province of Girona, Spain. The study's key goals include creating a comprehensive bank of images through Magnetic Resonance Imaging, establishing an ageing atlas of the human body, and discovering new imaging biomarkers that could predict disease onset (24).

The aim of our study is to extend the current knowledge regarding the connection between morphological and functional changes in the heart associated with ageing, in relation to the degree of cerebral atrophy and the presence of white matter hyperintensities. The identification of relationships, if established, would contribute to a deeper comprehension of the intricate heart-brain axis. Furthermore, it could facilitate the formulation of preventive strategies aimed at mitigating the onset of specific neurologic diseases like dementia.

5. HYPOTHESES

5.1. MAIN HYPOTHESES

- In the ageing population, **morphological changes in the left ventricle** are associated with cerebral damage, specifically with the presence of **white matter lesions** evaluated through MRI imaging studies.
- **Morphological changes in the left ventricle** associated with ageing correlate with the **degree of cerebral atrophy** as assessed through MRI imaging studies.

5.2. SECONDARY HYPOTHESES

- **Functional left ventricle changes** related to ageing, are associated with the appearance of **white matter lesions** evaluated through MRI imaging studies.
- **Functional left ventricle changes** related to ageing, are associated with the **degree of cerebral atrophy evaluated** through MRI imaging studies.
- **Right ventricle morphological and functional changes** related to ageing, are correlated with the appearance of **white matter lesions** evaluated through MRI imaging studies.
- **Right ventricle morphological and functional changes** related to ageing, correlate with the **degree of cerebral atrophy** as assessed through MRI imaging studies.

6. OBJECTIVES

6.1. MAIN OBJECTIVES

- The aim of this study is to assess if the **morphological changes in the left ventricle** related to ageing, are associated to the presence of **white matter lesions** evaluated through MRI imaging studies.
- This study aims to investigate if the **morphological left ventricle changes** related to ageing, are associated to the **degree of cerebral atrophy** as evaluated in MRI imaging studies.

6.2. SECONDARY OBJECTIVES

- To analyse if the **functional left ventricle changes** related to ageing, are connected to the appearance of **white matter lesions** evaluated through MRI imaging studies.
- To review if the **functional left ventricle changes** related to ageing, are connected to the **degree of cerebral atrophy** evaluated through MRI imaging studies.
- To assess if the **right ventricle morphological and functional changes** related to ageing, correlate with the identification of **white matter lesions** evaluated through MRI imaging studies.
- To examine whether **morphological and functional alterations in the right ventricle** due to ageing, are linked to the **degree of cerebral atrophy** as assessed in MRI imaging studies.

7. MATERIAL AND METHODS

7.1. STUDY DESIGN

This project is designed as an observational, analytical, transversal, prospective and individual study, with data from the population study “The Aging Imageomics”. Data was gathered in the Girona province spanning from 2017 to 2019. An analysis will be conducted on MRI studies of a group consisting of 1,030 participants to investigate the potential correlation between ageing in the heart and the brain.

7.2. STUDY POPULATION AND SAMPLING

The study's target population comprises individuals aged 50 years or older who are enrolled in The Aging Imageomics Study, constituting a group of around 1,030 people. This participants come from two independent ongoing cohort studies with their own eligibility criteria of individuals residing in the province of Girona, Spain: the Maturity and Satisfactory Ageing in Girona study (MESGI50 study) and the Improving interMediAte Risk management study (MARK study) (24).

The MARK study selected a random population of 2,688 people aged 35 to 74 from the province of Girona, Spain. The surveyed population exhibited an intermediate cardiovascular risk, ranging between 5-15% at 10 years, as per the Framingham adapted risk equation. The primary goal was to pinpoint individuals facing a high-risk scenario for cardiovascular disease, where primary preventive measures prove effective and efficient. Additionally, the study aspires to refine these predictions for greater precision, fostering a clinical and welfare impact on both health systems and citizens (53).

Their exclusion criteria were the presence of terminal illness or institutionalization at the appointment time, or a personal history of atherosclerotic disease (53).

The MESGI50 study is associated with a European Commission research initiative known as the Survey of Health, Aging, and Retirement in Europe (SHARE). Its purpose is to gather indicators of the ageing process in Europe. In this instance, they conducted a random selection of 28 municipalities within the province of Girona, Spain. The final

sample comprised 2,065 households and 3,331 participants aged 50 years or older. Their aim was to comprehend the demographic, health, and socioeconomic characteristics throughout the ageing process, examining potential differences based on age groups, gender, and area of residence (54).

Inclusion criteria involved being born in 1962 or earlier, and being officially registered and habitually residing in the municipality. Exclusion criteria included individuals in prison or hospitalized, those residing in geriatric centres, individuals with language barriers, or those with an unknown address due to a change of residence (54).

Individuals from both cohorts were contacted via telephone to extend an invitation to participate in The Aging Imageomics Study. In the course of this standardized telephone communication, prospective candidates received comprehensive information about the study and were prompted to seek more detailed clarification if desired. Those who expressed willingness to participate were then prompted to select a suitable date and time for the completion of the enrolment procedures (24).

7.2.1. Inclusion criteria

- Participants must be aged 50 years or older.
- Signing of the informed consent.

7.2.2. Exclusion criteria

- History of infection in the last 15 days.
- Contraindications for performing an MRI⁶.

Also, participants could consent to be informed of potential incidental findings, but it was not a mandatory criteria for joining the study.

⁶ The following are considered absolute contraindications for MRI: (1) Cardiac electronic devices, (2) Cochlear implants, (3) Non-MRI compatible cardiac valve prostheses, (4) Non-MRI compatible vascular clips, (5) Metallic foreign bodies in eyes and other life-threatening places, (6) Any type of circumstance that may make it impossible to perform the MRI scan (claustrophobia).

7.3. STUDY PROCEDURES

The data collection for the Imageomics project occurred from November 14, 2017, to June 19, 2019. Participants underwent two scheduled appointments. The initial visit comprised three segments. Firstly, participants received detailed information about the study's objectives and characteristics. Secondly, those who provided informed written consent were assigned a personal identification code and subsequently underwent whole-body MRI and carotid ultrasound studies. Thirdly, participants were scheduled for a subsequent examination 15 days later. At this point, a research assistant provided a kit along with detailed step-by-step instructions for collecting and transporting morning urine and stool samples to be presented on the day of the following visit.

The second visit involved three components. Firstly, morning urine and stool samples were collected, and blood samples were drawn between 8:00 a.m. and 10:00 a.m. After basic processing, specimens were transported to the Institut d'Investigació Biomèdica de Girona (IDIBGI) Biobank central laboratory via a cold chain, and then frozen at -80°C for future use. Secondly, participants underwent an anthropometric examination, a clinical interview, and a cardiovascular examination conducted by a trained nursing team. Thirdly, participants completed standardized tests and questionnaires administered by the nursing team and trained psychology students to measure cognitive, mood, and personality-related variables. Participants from the MARK study were also invited to further collaborate by using a device to measure ambient air pollution in the 2 weeks between visits.

Upon the conclusion of the study, participants were provided with a comprehensive report outlining the key findings from the MRI, carotid ultrasound, electrocardiogram, and blood test.

7.4. WHOLE-BODY MRI ACQUISITION PROTOCOL

At the initiation of the study, MRI examinations were conducted utilizing a portable 1.5 Tesla Vantage Elan scanner manufactured by Toshiba Medical Systems, now from Canon Medical Systems. The setup involves employing a head coil and two body coils to cover

the entire body, with a maximum gradient amplitude of 35mT/m-1. In summary, the acquisition protocol incorporates various sequences designed to examine distinct anatomical regions, including the thoracoabdominal region, brain, heart, aortic flow, abdominal aorta and iliac segments, as well as the abdomen and the entire spine (24). Figure 6 shows a graphic representation of each of the acquisitions.

Four medical imaging technologists were engaged in MRI acquisition. They underwent an extensive one-month training program on the imaging platform offered by the vendor, supplemented by additional training. These technologists conducted visual assessments of the image quality obtained throughout the acquisition process. Additionally, a dedicated MRI physicist and a radiologist independently reviewed subsets of the images to verify compliance with acquisition standards (24).

Cardiac images were acquired with electrocardiographic synchronization. Initially, a long-axis view (equivalent to a two-chamber) was obtained, followed by a short-axis view from the base to the apex of the left ventricle. This sequential approach facilitated the volumetric study. The imaging sequence employed was the short-axis cine steady-state free precession (SSFP). SSFP is known for producing high-quality images, particularly of the myocardium. The cine capability enables a precise calculation of the ventricle volumes, eliminating the need for making geometric assumptions as required in ultrasound studies (55).

In the study of the brain, five distinct sequences were employed, with our choice being the T2-weighted sequence using magnetization-prepared rapid acquisition gradient echo (MP RAGE). This sequence is renowned for its ability to yield excellent contrast, especially distinguishing between grey matter and white matter, and producing high-resolution three-dimensional images (56).

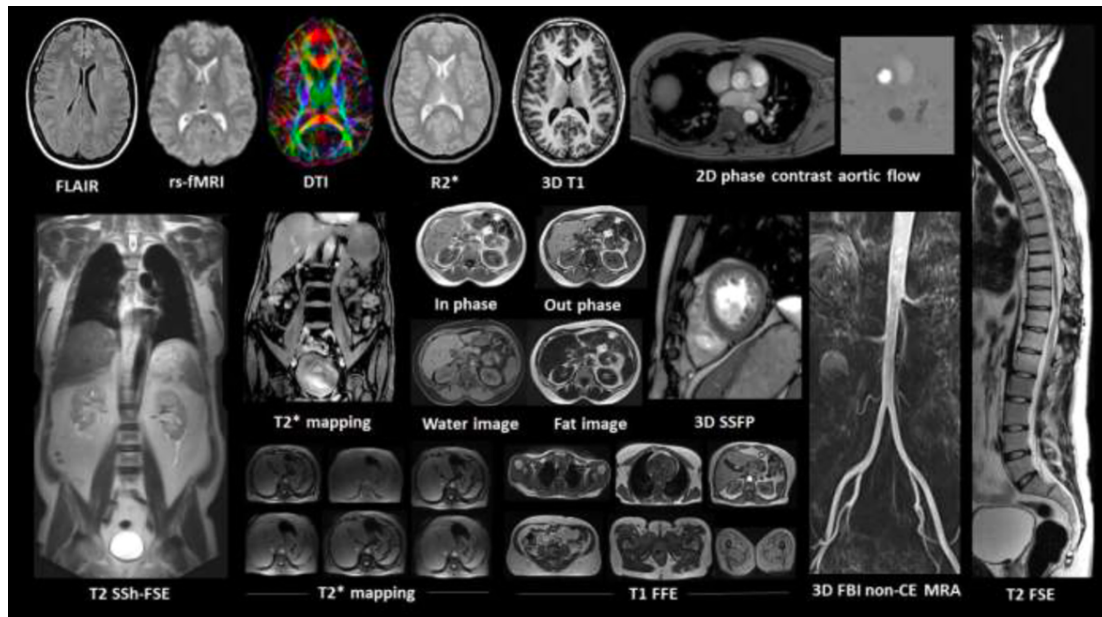


Figure 6 – Ageing resonance imaging acquisition protocol from the Imageomics Study.

Abbreviations: DTI: Diffusion tensor imaging, FLAIR: Fluid attenuation inversion recovery, rsfMRI: Resting-state functional magnetic resonance imaging, SSFP: Steady-state free precession, SSh-FSE: Single-shot fast spin echo, TSE: Turbo spin echo. *Source: The Ageing Imageomics Study (24).*

7.5. CAROTID ULTRASOUND STUDY

A radiologist conducted all carotid ultrasound examinations using a Siemens Acuson S2000 system equipped with a 7.5 MHz linear array transducer. The assessment involved measuring the percentage of carotid stenosis on B-mode, focusing on the common carotid artery and internal carotid artery. Following the capture of a transverse scan of the most stenotic segment, both the original diameter and residual diameter were determined using electronic callipers (24).

The residual diameter was defined as the shortest diameter of the residual lumen at the most stenotic carotid segment. In contrast, the original diameter was defined as the measured diameter from the outer media to the outer media of the diseased artery, within the same plane and direction as the residual diameter. This value was calculated using the following equation: Carotid stenosis percentage = $(1 - [\text{residual diameter}/\text{original diameter}]) \times 100$, as previously described. The carotid intima–media thickness and plaques will be measured according to the Mannheim Consensus (24).

7.6. VARIABLES

7.6.1. Main variables

- **Independent variables:** Morphological changes in the left ventricle. We included the following as morphological variables:
 - Left ventricle end-diastolic mass: It is a continuous quantitative variable expressed in grams (g) / square meter (m²).
 - Left ventricle end-diastolic volume: It is a continuous quantitative variable expressed in millilitres (ml) / m².
 - Left ventricle end-systolic volume: It is a continuous quantitative variable expressed in ml/m².
 - Mass/volume index of the left ventricle: It is a continuous quantitative variable expressed in g/ml.

- **Dependent variables:** Appearance of white matter lesions and the degree of cerebral atrophy.
 - White matter lesions: It is a continuous quantitative variable expressed in ml.
 - Degree of cerebral atrophy: We used four segmentations to study the atrophy:
 - Total cortex volume: It is a continuous quantitative variable expressed in ml.
 - Total brain volume without the ventricles: It is a continuous quantitative variable expressed in ml.
 - Volume of grey matter: It is a continuous quantitative variable expressed in ml.
 - Volume of cortical white matter: It is a continuous quantitative variable expressed in ml.

7.6.2. Secondary variables

- **Functional left ventricle changes:**
 - Left ventricle ejection fraction: It is a continuous quantitative variable expressed as a %.
 - Left ventricle stroke volume: It is a continuous quantitative variable expressed in ml/m².
 - Left ventricle cardiac output: It is a continuous quantitative variable expressed in litres (l) / (minutes*m²).
 - Global longitudinal endocardial strain: It is a continuous quantitative variable expressed as a %.
 - Global circumferential endocardial strain: It is a continuous quantitative variable expressed as a %.
 - Global radial strain: It is a continuous quantitative variable expressed as a %.

- **Right ventricle variables:**
 - Morphological:
 - Right ventricle end-diastolic volume: It is a continuous quantitative variable expressed in ml / m².
 - Right ventricle end-systolic volume: It is a continuous quantitative variable expressed in ml / m².

 - Functional:
 - Right ventricle ejection fraction: It is a continuous quantitative variable expressed as a %.
 - Right ventricle stroke volume: It is a continuous quantitative variable expressed in ml/m².

7.6.3. Covariates

- **Age:** Quantified in years from the time of birth. It is a discrete quantitative variable.

- **Sex:** Categorized as male or female. It is a qualitative dichotomous variable.
- **Degree of carotid stenosis:** Measured with an ultrasound [See section 7.5. “Carotid ultrasound study”]. It was divided in three groups: normal, asymptomatic stenosis (less than 70% occlusion) and symptomatic stenosis (70% or more). It is a qualitative ordinal variable.

7.7. DATA HANDLING AND STORAGE

All the data from The Aging Imageomics project was codified and stored in accordance with “*Ley Orgánica 3/2018, de 5 de diciembre, de Protección de Datos Personales y garantía de los derechos digitales*”. Two databases were employed, with participants' names and study identification codes inputted using individual passwords in an encrypted database.

Information from questionnaires and medical devices was recorded in a separate anonymous electronic database, utilizing the personal study identification code. A data manager reviewed entries for completeness and plausibility, making corrections for incomplete or implausible data when feasible. Additional data from biological samples and MRI postprocessing were linked via the personal study identification code. Regularly, encrypted backups of both databases were stored on two external hard disks located at different sites (24).

7.8. FIELDWORK

In order to acquire the necessary data from cardiac and brain MRI scans, post-processing of all the imaging was essential. The Imageomics team had already processed the brain MRIs using the FreeSurfer software package. The variables extracted from the segmentations included white matter hyperintensities, cortex volume, total grey matter volume, total cortical white matter volume, and brain volume excluding the ventricles.

On the other hand, our primary task revolved around segmenting the cardiac MRI images for all participants. Employing the Medis Suite MR Medical Imaging software, we devised a systematic approach to ensure that both my colleague and I analysed distinct parameters in the same sequence.

Initially, we began with the short axis of the heart, verifying the accurate delineation of the myocardium and endocardium of the left ventricle, along with the right ventricle. Subsequently, we selected basal, mitral, and apical sequences to conduct left ventricle strain analysis.

Upon completing the short axis assessment, we proceeded to the long axis study, acquiring information about the left ventricle ejection fraction and strain. Additionally, we gathered data on the volumes and strain of the left atrium.

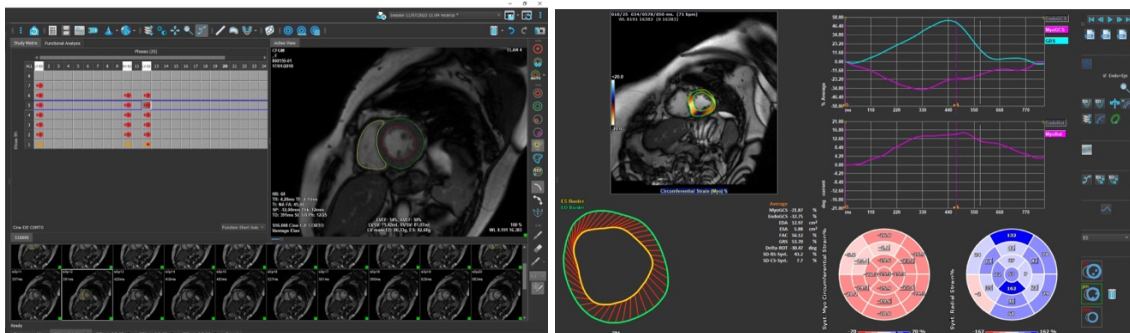


Figure 7 (A and B) – Segmentation of the short axis.

Figure 7A (left) shows the left ventricle myocardium delineated in green, the endocardium in red, and the right ventricle in yellow. Figure 7B (right) displays the strain of the short axis after selecting basal, mitral, and apical sequences.

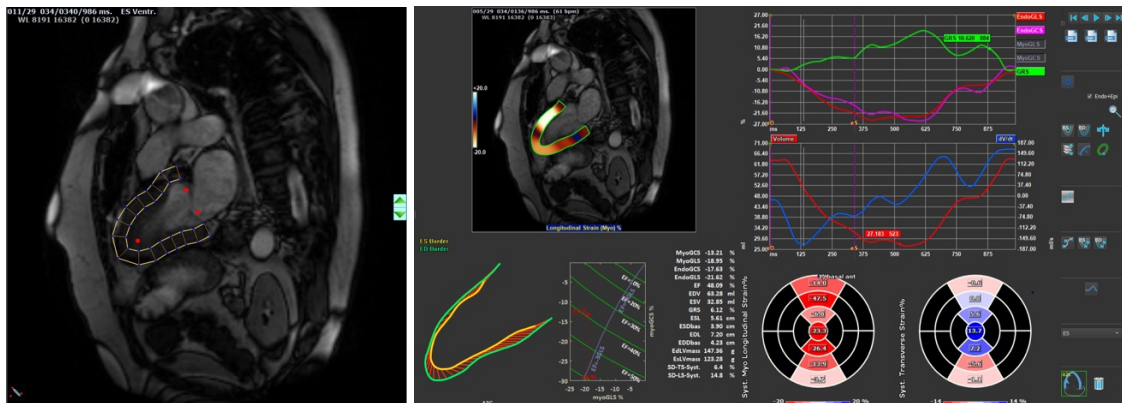


Figure 8 (A and B) – Segmentation of the long axis.

In Figure 8A (left), the left ventricle long axis is delineated. After this delineation, Figure 8B (right) illustrates the strain of the left ventricle long axis.

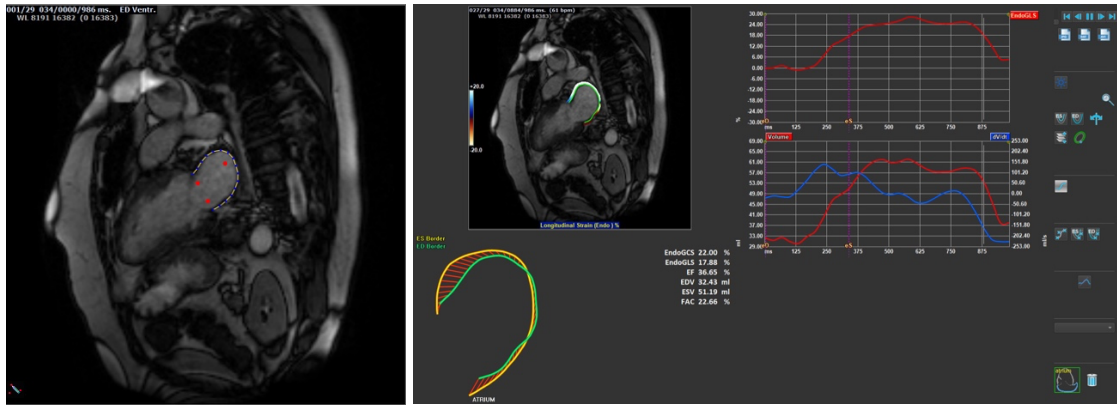


Figure 9 (A and B) – Segmentation of the atrium.

Figure 9A (left) depicts the delineation of the left atrium for the purpose of obtaining information about its volumes. Figure 9B (right) illustrates the strain of the left atrium.

The post-processing of MRI sequences plays a pivotal role in converting the wealth of information obtained from MRI scans into analysable data. The integration of artificial intelligence techniques, particularly those rooted in *Machine learning*, into both brain and heart post-processing software has significantly enhanced analysis. AI contributes to minimizing variability among operators, enhancing the quality of segmentations, and enabling a quicker and more precise examination of all imaging data.

7.9. STATISTICAL ANALYSIS

The statistical analysis was conducted utilizing the R software⁷ version 4.3.1 for Windows. A p-value lower than 0.05 was established as statistically significant, and the confidence intervals were computed at the 95% of confidence level in all analyses. In descriptive tables, continuous data were presented as mean \pm standard deviation (SD), while categorical data were presented as counts and percentages.

- Descriptive analysis

Demographic and health characteristics of participants were examined to identify distinctions between men and women. To assess the differences for continuous quantitative variables, either Student's t-test or Welch's t-test were used, based on the assumption of equal variances between men and women. If variances could be

⁷ The R software is an open-source environment for statistical computing and graphics, created by The R Foundation for Statistical Computing in Vienna, Austria.

considered to be equal, Student's t-test was employed; otherwise, Welch's t-test was utilized.

For categorical variables, either the chi-square test of independence or Fisher's exact test was employed. Fisher's exact test was specifically utilized when dealing with contingency tables containing cells with limited observations.

- **Bivariate analysis**

We utilize simple linear regression models to assess the relationship between two quantitative variables. In our study, we examine the associations between heart morphology variables as predictors (independents) and various brain measures as predicted (dependent). Each coefficient in the regression equation is derived from a distinct model, as each regression analyses a single measure of the brain in conjunction with a single measure of the heart.

The coefficients are understood as the alteration in the predicted variables (specifically, various brain measures) for every one-unit increment in the predictor variables (distinct measures of heart morphology).

- **Multivariate analysis**

To mitigate potential confounding we accounted for covariates by adjusting the coefficients of the linear regression models for age, sex, and the degree of carotid stenosis. First, we adjusted individually for each variable, and then collectively for all three of them.

7.10. ETHICAL CONSIDERATIONS

The Aging Imageomics Study protocol was approved by the Clinical Research Ethics Committee (CEIC) from Hospital Universitari Doctor Josep Trueta, on October 27th 2017. As it can be seen in "Annex 1", the CEIC states that documents conform to the essential ethical standards and has therefore decided to approve them.

Adhering to human rights and ethical principles, the study aligns with the 64th Declaration of Helsinki by the World Medical Association, last revised in October 2013.

Furthermore, it complies with the principles outlined in the Belmont Report, emphasizing autonomy, justice, beneficence, and non-maleficence.

To uphold the principle of autonomy, the study honoured the values and personal choices of each participant throughout the research. An information sheet detailing the study protocol [see “Annex 2”] was presented in a comprehensible language and explained by a member of the study team. Additionally, a contact number was provided for any further inquiries or concerns that participants might have had.

Investigators obtained written informed consent from each participant before their participation in the study [see “Annex 3”]. Participants were informed that they have the freedom to decline participation in the study and are at liberty to withdraw at any time without facing any negative consequences. Moreover, individuals had the option to decline being informed about potential incidental findings [see “Annex 4”].

8. RESULTS

The final study cohort comprised 1,030 participants, with 567 (55.0%) recruited from the MARK study and 463 (45.0%) from the MESGI study. Figure 10 delineates the inclusion process in the study through a flowchart. The mean age was 66.81 ± 7.08 , with a population ranging between 50 and 98 years, consisting in 53.6% men and 46.4% women.

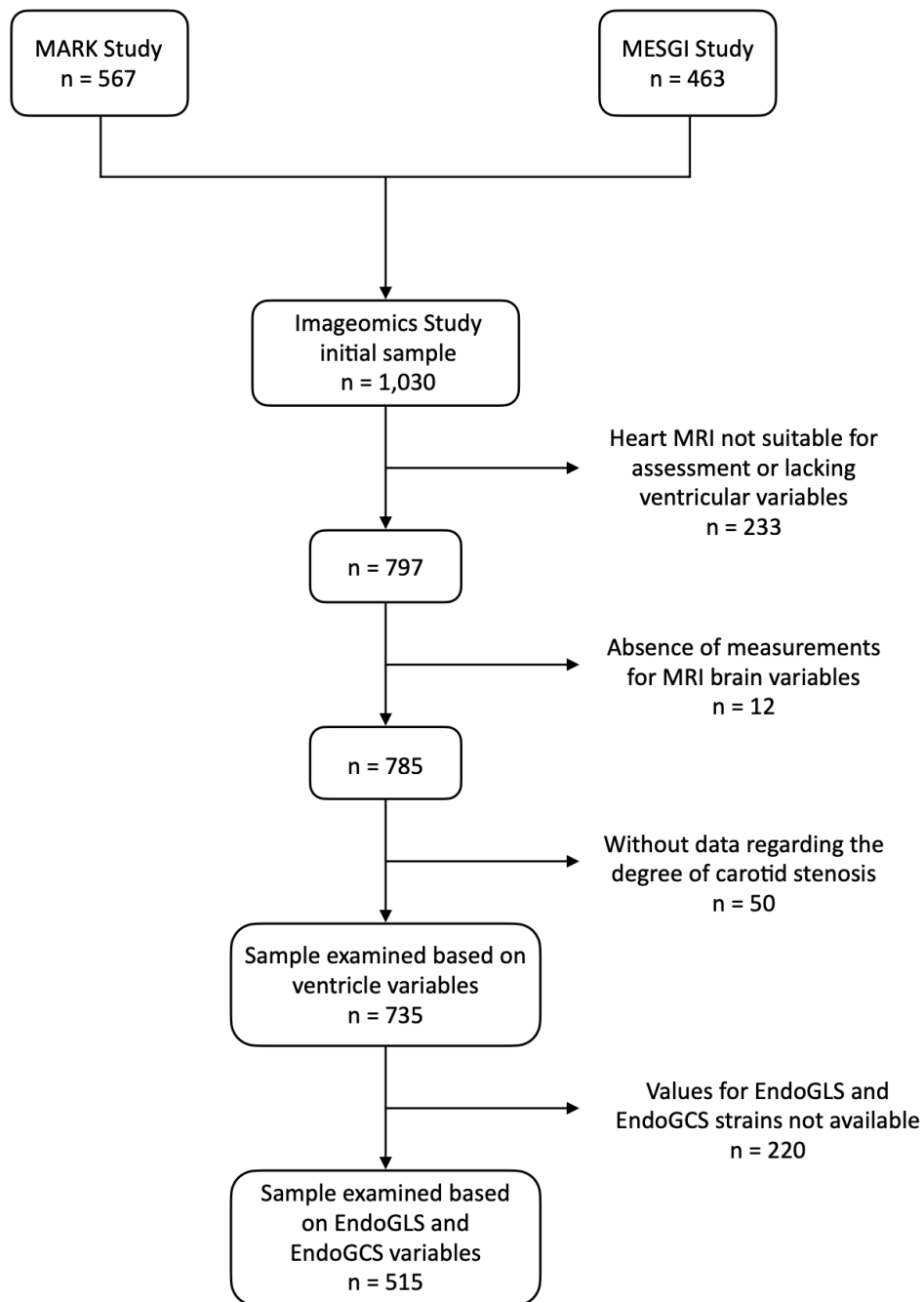


Figure 10 – Flowchart of our study

Abbreviations: MRI: Magnetic resonance imaging, EndoGLS: Endocardial Global longitudinal strain, EndoGCS: Endocardial Global circumferential strain.

As evident in Table 1, educational level was categorized as up to primary in 56.97%, secondary in 31.31%, and university in 11.72%, with a slightly higher level among men. This difference can likely be attributed to the historical period and societal norms of that era, wherein women did not had the same opportunities as men. Within our sample, 70.90% had already retired, with a slightly higher proportion observed in men. Women exhibited a higher rate of unemployment or sickness at 8.01%, compared to 4.38% in men.

In terms of risk factors, men exhibited a higher prevalence of high blood pressure history, while women had a more significant family history of cardiovascular disease. The mean systolic blood pressure was over 140mmHg in both genders, and the diastolic pressure approached nearly 90mmHg. Additionally, the rate of symptomatic stenosis was higher in men compared to women.

Both genders primarily demonstrated a moderate adherence to the Mediterranean diet. The majority of male participants belonged to the high physical activity group, while most female participants were in the moderate activity group. A significant proportion, surpassing 80% of both male and female study participants, reported being non-smokers.

Table 1: Demographic, health and social characteristics.

Variables	Category	Total sample	Female	Male	p-value
Participants, mean (SD)		735	341	394	
Age, mean (SD)		66.81 (7.08)	66.26 (7.45)	67.29 (6.72)	0.050
Education level, n (%)	Up to primary	413 (56.97)	204 (60.36)	209 (54.01)	0.211
	Secondary	227 (31.31)	99 (29.29)	128 (33.07)	
	University	85 (11.72)	35 (10.36)	50 (12.92)	

Working status, n (%)	Retired	514 (70.90)	228 (67.66)	286 (73.71)	0.070
	Employed	167 (23.03)	82 (24.33)	85 (21.91)	
	Other (unemployed/sick)	44 (6.07)	27 (8.01)	17 (4.38)	
History of HBP, n (%)		331 (45.53)	141 (41.59)	190 (48.97)	0.055
Systolic pressure, mean (SD)		148.43 (19.39)	149.55 (21.04)	147.48 (17.85)	0.151
Diastolic pressure, mean (SD)		89.40 (9.87)	87.78 (9.82)	90.78 (9.72)	p<0.001
History of Diabetes, n (%)		156 (21.43)	70 (20.65)	86 (22.11)	0.698
History of dyslipidaemia, n (%)		201 (27.61)	89 (26.25)	112 (28.79)	0.496
Total cholesterol, mean (SD)		197.82 (34.83)	205.75 (33.11)	190.99 (34.87)	p<0.001
HDL cholesterol, mean (SD)		53.50 (15.81)	59.08 (16.59)	48.70 (13.38)	p<0.001
LDL cholesterol, mean (SD)		120.56 (30.98)	123.21 (30.53)	118.26 (31.23)	0.034
Fasting TGL, mean (SD)		121.31 (74.31)	117.55 (60.54)	124.55 (84.34)	0.211
Smoke, n (%)		113 (15.61)	46 (13.73)	67 (17.22)	0.235
Physical activity, n (%)	High	341 (48.85)	132 (40.99)	209 (55.59)	p<0.001
	Moderate	300 (42.98)	159 (49.38)	141 (37.50)	
	Low	57 (8.17)	31 (9.63)	26 (6.91)	
Mediterranean diet adherence, n (%)	High	221 (31.66)	105 (32.61)	116 (30.85)	0.878
	Moderate	419 (60.03)	105 (32.61)	116 (30.85)	
	Low	58 (8.31)	26 (8.07)	32 (8.51)	
History of Cardiac failure, n (%)		9 (1.24)	4 (1.19)	5 (1.28)	1.000
History of AFib, n (%)		12 (1.66)	7 (2.08)	5 (1.29)	0.561

Personal history CVD, n (%)		117 (16.07)	52 (15.43)	65 (16.62)	0.737
Family history CVD, n (%)		275 (38.25)	146 (44.11)	129 (33.25)	0.004
Carotid US examinations, n (%)	Normal	283 (38.50)	164 (48.09)	119 (30.20)	p<0.001
	Asymptomatic stenosis (<70%)	383 (52.11)	156 (45.75)	227 (57.61)	
	Symptomatic stenosis (>=70%)	69 (9.39)	21 (6.16)	48 (12.18)	

Abbreviations: SD: Standard deviation, HBP: High blood pressure, HDL: High-density lipoprotein , LDL: Low-density lipoprotein, TGL: Triglycerides , AFib: Atrial fibrillation, CVD: Cardiovascular disease, US: Ultrasound.

Table 2 summarizes the heart's morphological and functional variables, as well as the relevant brain variables considered for analysis. To gain a deeper comprehension of the study, it is essential to clarify specific parameters. Ejection fraction represents the percentage of blood expelled from the left ventricle during each contraction. Stroke volume denotes the volume of blood ejected by the left ventricle in a single contraction or heartbeat. Cardiac output measures the quantity of blood pumped by the heart within a given time unit, determined by multiplying the stroke volume with the heart rate (57).

Table 2: Variables related to heart morphology, function, and brain parameters.					
Variables	Units	Total sample	Female	Male	p-value
LV end-diastolic mass ^{BS} , mean (SD)	g/m ²	46.06 (9.16)	42.99 (7.61)	48.71 (9.55)	p<0.001
LV end-diastolic volume ^{BS} , mean (SD)	ml/m ²	62.91 (15.14)	60.09 (13.34)	65.34 (16.16)	p<0.001
LV end-systolic volume ^{BS} , mean (SD)	ml/m ²	23.47 (9.73)	21.81 (8.91)	24.90 (10.18)	p<0.001
LV mass/volume index ^{BS} , mean (SD)	g/ml	0.75 (0.15)	0.73 (0.13)	0.77 (0.17)	p<0.001
LV ejection fraction, mean (SD)	%	63.38 (9.26)	64.42 (8.84)	62.48 (9.52)	0.004
LV stroke volume ^{BS} , mean (SD)	ml/m ²	39.44 (9.40)	38.28 (8.16)	40.44 (10.26)	0.002

LV cardiac output ^{BS} , mean (SD)	l/ (min* m ²)	2.69 (0.64)	2.63 (0.57)	2.75 (0.70)	0.008
LV Global longitudinal strain, mean (SD)	%	-18.56 (5.75)	-19.17 (5.85)	-17.95 (5.60)	0.016
LV Global circumferential strain, mean (SD)	%	-25.83 (10.91)	-27.01 (10.58)	-24.66 (11.13)	0.015
LV Global radial strain, mean (SD)	%	68.25 (41.27)	66.45 (30.12)	69.80 (48.90)	0.273
RV end-diastolic volume ^{BS} , mean (SD)	ml/m ²	62.51 (15.72)	56.46 (12.12)	67.75 (16.59)	p<0.001
RV end-systolic volume ^{BS} , mean (SD)	ml/m ²	25.83 (8.94)	21.82 (6.71)	29.31 (9.17)	p<0.001
RV ejection fraction, mean (SD)	%	58.61 (10.36)	61.16 (9.67)	56.41 (10.45)	p<0.001
RV stroke volume ^{BS} , mean (SD)	ml/m ²	36.68 (11.02)	34.64 (9.41)	38.44 (11.98)	p<0.001
White matter hyperintensities, mean (SD)	ml	3.85 (3.22)	3.15 (2.15)	4.46 (3.82)	p<0.001
Cortex volume, mean (SD)	ml	362.83 (37.11)	346.15 (32.29)	377.27 (34.91)	p<0.001
Cortex volume without ventricles, mean (SD)	ml	995.60 (105.56)	945.37 (94.01)	1,039.06 (95.29)	p<0.001
Cortical white matter volume, mean (SD)	ml	463.40 (63.53)	435.46 (56.48)	487.58 (59.29)	p<0.001
Total grey matter volume, mean (SD)	ml	507.07 (46.13)	485.56 (41.05)	525.68 (42.06)	p<0.001

Variables marked with a BS superscript have been normalized by body surface (BS) area. Abbreviations: LV: Left ventricle, RV: Right ventricle, SD: Standard deviation.

8.1. BIVARIATE ANALYSIS

Table 3 displays the unprocessed outcomes of the simple linear regression test conducted between the heart and brain variables. Notably, several correlation coefficients have achieved statistical significance. However, upon adjustment for covariates [see “Table 4”], the majority of these correlations no longer maintain statistical significance.

Table 3: Unprocessed findings from the comparison of variables between the heart and brain.

Variables	WMH	Cortex volume	Cortex volume without ventricles	Cortical white matter volume	Total grey matter volume
LV end-diastolic mass ^{BS} , mean (SD)	0.06 (0.03,0.08) [p<0.001]*	0.48 (0.19,0.77) [0.001]*	1.20 (0.36,2.03) [0.005]*	0.58 (0.08,1.09) [0.022]*	0.61 (0.25,0.98) [p<0.001]*
LV end-diastolic volume ^{BS} , mean (SD)	0.01 (-0.00,0.03) [0.095]	0.31 (0.14,0.49) [p<0.001]*	0.79 (0.29,1.29) [0.002]*	0.41 (0.10,0.71) [0.008]*	0.39 (0.17,0.61) [p<0.001]*
LV end-systolic volume ^{BS} , mean (SD)	0.01 (-0.01,0.04) [0.275]	0.37 (0.09,0.64) [0.009]*	0.93 (0.15,1.72) [0.019]*	0.50 (0.03,0.97) [0.039]*	0.44 (0.10,0.78) [0.012]*
LV mass/volume index ^{BS} , mean (SD)	1.94 (0.42,3.46) [0.013]*	-7.89 (-25.46,9.69) [0.379]	-17.96 (-67.97,32.05) [0.481]	-10.07 (-40.17,20.03) [0.512]	-8.29 (-30.14,13.57) [0.457]
LV ejection fraction, mean (SD)	-0.00 (-0.03,0.03) [0.988]	-0.18 (-0.47,0.11) [0.224]	-0.50 (-1.32,0.33) [0.238]	-0.27 (-0.76,0.23) [0.292]	-0.23 (-0.59,0.13) [0.215]
LV stroke volume ^{BS} , mean (SD)	0.02 (-0.01,0.04) [0.119]	0.42 (0.13,0.70) [0.004]*	1.05 (0.24,1.86) [0.011]*	0.52 (0.03,1.01) [0.036]*	0.53 (0.18,0.89) [0.003]*
LV cardiac output ^{BS} , mean (SD)	0.25 (-0.12,0.61) [0.182]	5.35 (1.19,9.52) [0.012]*	13.42 (1.56,25.27) [0.027]*	6.50 (-0.64,13.65) [0.074]	6.93 (1.75,12.10) [0.009]*
LV Global longitudinal strain, mean (SD)	0.05 (0.00,0.10) [0.045]*	0.11 (-0.45,0.67) [0.706]	0.63 (-0.97,2.22) [0.440]	0.26 (-0.69,1.22) [0.588]	0.34 (-0.36,1.04) [0.337]
LV Global circumferential strain, mean (SD)	0.02 (-0.01,0.05) [0.128]	0.14 (-0.15,0.44) [0.344]	0.44 (-0.39,1.28) [0.298]	0.18 (-0.33,0.68) [0.492]	0.25 (-0.12,0.62) [0.185]
LV Global radial strain, mean (SD)	0.00 (-0.00,0.01) [0.432]	0.01 (-0.06,0.08) [0.762]	0.11 (-0.08,0.29) [0.260]	0.07 (-0.04,0.18) [0.197]	0.03 (-0.05,0.11) [0.498]
RV end-diastolic volume ^{BS} , mean (SD)	0.00 (-0.01,0.02) [0.557]	0.56 (0.39,0.73) [p<0.001]*	1.44 (0.97,1.92) [p<0.001]*	0.69 (0.40,0.98) [p<0.001]*	0.73 (0.53,0.94) [p<0.001]*
RV end-systolic volume ^{BS} , mean (SD)	0.01 (-0.02,0.03) [0.607]	1.09 (0.80,1.38) [p<0.001]*	2.98 (2.15,3.81) [p<0.001]*	1.56 (1.06,2.06) [p<0.001]*	1.37 (1.01,1.73) [p<0.001]*
RV ejection fraction, mean (SD)	-0.00 (-0.03,0.02) [0.687]	-0.44 (-0.70,-0.18) [p<0.001]*	-1.37 (-2.11,-0.64) [p<0.001]*	-0.84 (-1.28,-0.40) [p<0.001]*	-0.50 (-0.82,-0.18) [0.002]*
RV stroke volume ^{BS} , mean (SD)	0.00 (-0.02,0.03) [0.674]	0.42 (0.18,0.67) [p<0.001]*	0.98 (0.29,1.67) [0.006]*	0.39 (-0.03,0.80) [0.069]	0.59 (0.29,0.89) [p<0.001]*

The coefficients marked with an asterisk (*) are statistically significant results. Variables marked with a BS superscript have been normalized by body surface (BS) area. Abbreviations: WMH: White matter hyperintensities, LV: Left ventricle, RV: Right ventricle, SD: Standard deviation

8.2. MULTIVARIATE ANALYSIS

Once adjustments were made for age, sex, and the degree of carotid stenosis as covariates, the statistically significant findings diminished. To determine which confounding variable was more closely linked to the loss of statistical significance, we individually adjusted for each of these covariates.

As seen in Table 4, upon adjusting for gender, we observed that most of the significant relationships disappeared. However, when adjusting for age and the degree of carotid stenosis, the coefficients did not change significantly [refer to “Annexes 5 and 6”].

Variables	WMH	Cortex volume	Cortex volume without ventricles	Cortical white matter volume	Total grey matter volume
LV end-diastolic mass ^{BS} , mean (SD)	0.04 (0.01,0.06) [0.005]*	-0.06 (-0.34,0.23) [0.699]	-0.44 (-1.23,0.35) [0.277]	-0.33 (-0.82,0.15) [0.177]	-0.07 (-0.42,0.27) [0.677]
LV end-diastolic volume ^{BS} , mean (SD)	0.01 (-0.01,0.02) [0.455]	0.14 (-0.02,0.30) [0.094]	0.27 (-0.19,0.73) [0.257]	0.11 (-0.17,0.40) [0.431]	0.16 (-0.04,0.37) [0.113]
LV end-systolic volume ^{BS} , mean (SD)	0.00 (-0.02,0.03) [0.818]	0.12 (-0.14,0.37) [0.360]	0.18 (-0.54,0.89) [0.625]	0.08 (-0.36,0.51) [0.733]	0.12 (-0.20,0.43) [0.464]
LV mass/volume index ^{BS} , mean (SD)	1.44 (-0.07,2.94) [0.061]	-20.63 (-36.67,-4.60) [0.012]*	-56.25 (-101.29,-11.21) [0.014]*	-31.37 (-58.98,-3.77) [0.026]*	-24.69 (-44.47,-4.91) [0.014]*
LV ejection fraction, mean (SD)	0.01 (-0.02,0.03) [0.568]	-0.00 (-0.27,0.26) [0.971]	0.03 (-0.72,0.78) [0.936]	0.03 (-0.43,0.48) [0.908]	-0.00 (-0.33,0.33) [0.989]
LV stroke volume ^{BS} , mean (SD)	0.01 (-0.01,0.04) [0.339]	0.23 (-0.03,0.49) [0.084]	0.49 (-0.25,1.22) [0.191]	0.21 (-0.24,0.66) [0.364]	0.29 (-0.03,0.61) [0.076]
LV cardiac output ^{BS} , mean (SD)	0.15 (-0.21,0.51) [0.411]	3.04 (-0.77,6.85) [0.118]	6.43 (-4.28,17.14) [0.239]	2.61 (-3.96,9.17) [0.436]	3.94 (-0.76,8.64) [0.100]
LV Global longitudinal strain, mean (SD)	0.04 (-0.01,0.09) [0.108]	-0.18 (-0.70,0.33) [0.479]	-0.25 (-1.69,1.18) [0.727]	-0.23 (-1.10,0.64) [0.608]	-0.03 (-0.67,0.61) [0.924]
LV Global circumferential strain, mean (SD)	0.02 (-0.01,0.04) [0.270]	-0.01 (-0.28,0.26) [0.929]	-0.02 (-0.78,0.73) [0.952]	-0.09 (-0.54,0.37) [0.716]	0.05 (-0.28,0.39) [0.765]

LV Global radial strain, mean (SD)	0.00 (-0.00,0.01) [0.565]	-0.01 (-0.06,0.05) [0.864]	0.06 (-0.11,0.23) [0.474]	0.05 (-0.05,0.15) [0.356]	0.01 (-0.06,0.08) [0.823]
RV end-diastolic volume ^{BS} , mean (SD)	-0.01 (-0.03,0.00) [0.133]	0.24 (0.07,0.40) [0.005]*	0.43 (-0.03,0.90) [0.068]	0.12 (-0.17,0.40) [0.429]	0.32 (0.11,0.52) [0.002]*
RV end-systolic volume ^{BS} , mean (SD)	-0.03 (-0.06,-0.00) [0.046]*	0.44 (0.14,0.74) [0.004]*	0.96 (0.12,1.80) [0.025]*	0.41 (-0.10,0.93) [0.118]	0.52 (0.15,0.89) [0.006]*
RV ejection fraction, mean (SD)	0.01 (-0.01,0.03) [0.374]	-0.10 (-0.34,0.14) [0.417]	-0.36 (-1.04,0.32) [0.299]	-0.28 (-0.70,0.13) [0.183]	-0.06 (-0.36,0.24) [0.705]
RV stroke volume ^{BS} , mean (SD)	-0.01 (-0.03,0.02) [0.589]	0.19 (-0.04,0.41) [0.104]	0.26 (-0.38,0.89) [0.427]	-0.02 (-0.41,0.37) [0.920]	0.29 (0.01,0.57) [0.041]*

The coefficients marked with an asterisk (*) are statistically significant results. Variables marked with a BS superscript have been normalized by body surface (BS) area. Abbreviations: WMH: White matter hyperintensities, LV: Left ventricle, RV: Right ventricle, SD: Standard deviation

The most notable outcome observed in Table 5 is the association between LV end-diastolic mass and the presence of WMH. For every gram increase in LV end-diastolic mass, there is a corresponding elevation of 0.04ml in the volume of WMH (CI: [0.01, 0.06], $p = 0.004$).

Additionally, the RV end-diastolic volume exhibits a positive correlation with the total grey matter volume (CI: [0.01, 0.40], $p = 0.042$). The RV end-systolic volume is associated with an augmentation in both the total grey volume (CI: [0.04, 0.75], $p = 0.027$) and the cortex volume (CI: [0.05, 0.62], $p = 0.022$). All these outcomes are presented in Table 5.

Table 5: Multivariate results adjusted for age, sex and degree of carotid stenosis.					
Variables	WMH	Cortex volume	Cortex volume without ventricles	Cortical white matter volume	Total grey matter volume
LV end-diastolic mass ^{BS} , mean (SD)	0.04 (0.01,0.06) [0.004]*	-0.04 (- 0.31,0.23) [0.756]	-0.43 (- 1.18,0.32) [0.261]	-0.33 (- 0.79,0.14) [0.171]	-0.07 (- 0.40,0.26) [0.662]
LV end-diastolic volume ^{BS} , mean (SD)	0.01 (- 0.00,0.03) [0.119]	0.08 (- 0.08,0.23) [0.340]	0.08 (- 0.36,0.52) [0.729]	0.02 (- 0.25,0.29) [0.891]	0.07 (- 0.12,0.27) [0.449]
LV end-systolic volume ^{BS} , mean (SD)	0.01 (- 0.01,0.03) [0.488]	0.06 (- 0.18,0.30) [0.618]	0.00 (- 0.68,0.68) [0.991]	-0.01 (- 0.43,0.41) [0.961]	0.03 (- 0.26,0.33) [0.822]
LV mass/volume index ^{BS} , mean (SD)	0.58 (- 0.88,2.03) [0.436]	-10.57 (- 26.03,4.89) [0.180]	-28.78 (- 72.11,14.55) [0.193]	-17.46 (- 44.47,9.54) [0.205]	-11.90 (- 30.83,7.03) [0.218]
LV ejection fraction, mean (SD)	0.00 (- 0.02,0.03) [0.704]	0.03 (- 0.23,0.28) [0.844]	0.12 (- 0.59,0.83) [0.743]	0.07 (- 0.37,0.51) [0.754]	0.04 (- 0.27,0.35) [0.804]
LV stroke volume ^{BS} , mean (SD)	0.02 (- 0.00,0.04) [0.077]	0.13 (- 0.12,0.38) [0.314]	0.19 (- 0.51,0.89) [0.589]	0.06 (- 0.38,0.50) [0.788]	0.15 (- 0.15,0.46) [0.329]
LV cardiac output ^{BS} , mean (SD)	0.27 (- 0.07,0.62) [0.118]	1.72 (- 1.92,5.37) [0.353]	2.49 (- 7.72,12.70) [0.633]	0.62 (- 5.74,6.99) [0.847]	2.09 (- 2.37,6.55) [0.358]
LV Global longitudinal strain, mean (SD)	0.03 (- 0.02,0.08) [0.216]	-0.06 (- 0.55,0.43) [0.815]	0.10 (- 1.27,1.47) [0.888]	-0.04 (- 0.88,0.81) [0.928]	0.12 (- 0.49,0.73) [0.697]
LV Global circumferential strain, mean (SD)	0.01 (- 0.01,0.04) [0.265]	-0.01 (- 0.27,0.25) [0.965]	-0.02 (- 0.74,0.71) [0.965]	-0.08 (- 0.53,0.36) [0.711]	0.06 (- 0.26,0.38) [0.719]
LV Global radial strain, mean (SD)	0.00 (- 0.00,0.01) [0.345]	-0.02 (- 0.07,0.04) [0.594]	0.03 (- 0.13,0.19) [0.705]	0.03 (- 0.07,0.13) [0.513]	-0.01 (- 0.08,0.06) [0.865]
RV end-diastolic volume ^{BS} , mean (SD)	-0.00 (- 0.02,0.01) [0.576]	0.15 (- 0.01,0.31) [0.072]	0.18 (- 0.26,0.63) [0.418]	-0.01 (- 0.29,0.27) [0.930]	0.20 (0.01,0.40) [0.042]*
RV end-systolic volume ^{BS} , mean (SD)	-0.02 (- 0.05,0.01) [0.141]	0.34 (0.05,0.62) [0.022]*	0.69 (- 0.11,1.49) [0.093]	0.27 (- 0.23,0.77) [0.284]	0.40 (0.04,0.75) [0.027]*
RV ejection fraction, mean (SD)	0.01 (- 0.01,0.04) [0.198]	-0.15 (- 0.38,0.08) [0.212]	-0.49 (- 1.14,0.15) [0.136]	-0.35 (- 0.75,0.05) [0.089]	-0.12 (- 0.40,0.16) [0.408]
RV stroke volume ^{BS} , mean (SD)	0.00 (- 0.02,0.02) [0.726]	0.08 (- 0.14,0.29) [0.479]	-0.05 (- 0.66,0.55) [0.866]	-0.18 (- 0.55,0.20) [0.356]	0.15 (- 0.12,0.41) [0.275]

The coefficients marked with an asterisk (*) are statistically significant results. Variables marked with a BS superscript have been normalized by body surface (BS) area. Abbreviations: WMH: White matter hyperintensities, LV: Left ventricle, RV: Right ventricle, SD: Standard deviation

9. DISCUSSION

Results from our study show a connection between left ventricle end-diastolic mass and white matter injury, observed as hyperintensities in the T2-weighted MRI sequence. The extent of injury consistently increased with the rise in left ventricle end-diastolic mass. However, no impact of functional and morphological left ventricle variables on the degree of cerebral atrophy was observed in any of the brain volumetric segmentations. These results align with prior knowledge, where changes in the mass of the left ventricle with age had been observed, but without alterations in ejection fraction. In our study, we also examined the strain as a more sensitive parameter than the ejection fraction, yet we did not observe changes in this aspect either.

Previous studies have done a tedious work demonstrating that, within our population, the increase in left ventricular mass aligns with the process of cardiac ageing. Also, the MESA, The Framingham Heart Study (33,34) and other studies, have identified cross-sectional and longitudinal associations between cardiovascular risk factors and cognitive decline, WMH and the degree of cerebral atrophy. Nevertheless, none of these studies had previously focused on directly correlating cardiac changes with those in the brain through MRI.

In our study, we observed that changes due to cardiac ageing, using the increase in cardiac mass as a surrogate parameter, correlate with the amount of WMH. Therefore, we demonstrate a relationship between cardiac ageing and cerebral ageing.

Upon a more in-depth analysis of the connection between the left ventricular end-diastolic mass and WMH, it is important to take into account that arterial hypertension might be linked to this result. Ageing involves a reduction in the elasticity and distensibility of large and medium-sized arteries, causing an augmentation in their rigidity and a rise in peripheral vascular resistance (58). Consequently, this leads to an increase in afterload, resulting in a concentric ventricular hypertrophy to compensate for this increased pressure against which the heart has to work (59).

Therefore, it is plausible that poorly controlled blood pressure is the cause of white matter lesions and the left ventricle's mass upsurge. This could explain the statistically

significant association we have identified between these two parameters, though it is crucial to acknowledge that the mechanisms behind ventricular hypertrophy are intricate and not fully understood.

This result, in a world that is gradually changing from disease treatment to prevention of the occurrence and development of ageing-related diseases, can have its importance. As it would suggest, effective blood pressure management might mitigate white matter lesion burden, which is associated with the onset of cognitive decline and dementia. Additionally, it could reduce left ventricular mass, which carries clinical implications such as heart failure, arrhythmias or myocardial infarction (60).

The most curious result to emerge from the data is the connection between right ventricle end-systolic and end-diastolic volumes and increased total grey matter volumes. Also, right ventricle end-systolic volume was also associated with raised total cortex volume.

The literature has not extensively examined the right ventricle and its relationship with the brain, so there are no available studies to compare our result; although it could be a very interesting field of research for future studies. From our perspective, and awaiting further investigation into potential significance, we can conclude that individuals with higher right ventricular volumes, within the normal range, exhibit a greater total volume of grey matter.

10. STUDY LIMITATIONS

The current study possesses certain limitations that should be acknowledged:

- **MRI acquisition:**

At certain points in the day while implementing the MRI protocol, technical difficulties were encountered with electrocardiographic synchronization necessary for acquiring heart MRI sequences. This occasionally resulted in the inability to capture the required sequences, or the obtained quality was insufficient for study purposes. This partly accounts for the absence of ventricular variables or the exclusion of 233 participants from assessment. It is important to note that the occurrence of these technical issues was entirely random and did not selectively impact any specific group of participants, thereby avoiding the introduction of bias in the studied population.

- **Sample:**

Population studies require a large amount of sample in order to obtain statistically significant results. Although our sample was not precisely small, especially considering the technical and economic effort involved, other studies include a larger sample size. The larger the sample, the greater statistical power the study has, and consequently, a higher probability of obtaining results and drawing conclusions. In our study, this could have caused certain trends that appeared in the results to emerge as significant findings. Moreover, the voluntary engagement in MRI studies frequently exhibits bias, as individuals in better health are more inclined to participate, especially within samples of older adults.

11. CONCLUSIONS

To sum up, the results of this study show a significant association between left ventricle mass and white matter hyperintensities. While functional and morphological left ventricle variables did not impact cerebral atrophy, our focus on heart-brain connections adds a unique dimension to existing research. Also, we did not find an association between functional left and right ventricle changes and white matter hyperintensities.

Additionally, our exploration of right ventricle volumes suggests a potential link to increased total grey matter, offering a novel perspective for future investigations. The significance of these findings lies in the potential for targeted interventions to mitigate white matter lesions by reducing cardiovascular risks.

12. BIBLIOGRAPHY

1. Clouston SAP, Brewster P, Kuh D, Richards M, Cooper R, Hardy R, et al. The Dynamic Relationship Between Physical Function and Cognition in Longitudinal Aging Cohorts. *Epidemiol Rev.* 2013;35(1):33–50.
2. Simm A, Nass N, Bartling B, Hofmann B, Silber RE, Navarrete Santos A. Potential biomarkers of ageing. *Biol Chem.* 2008 Mar;389(3):257–65.
3. World Health Organization [Internet]. [cited 2023 Sep 20]. Ageing and health. Available from: <https://www.who.int/news-room/fact-sheets/detail/ageing-and-health>
4. Niccoli T, Partridge L. Ageing as a Risk Factor for Disease. *Curr Biol.* 2012 Sep 11;22(17):R741–52.
5. Singh-Manoux A, Kivimaki M, Glymour MM, Elbaz A, Berr C, Ebmeier KP, et al. Timing of onset of cognitive decline: results from Whitehall II prospective cohort study. *BMJ.* 2012 Jan 5;344:d7622.
6. Guo J, Huang X, Dou L, Yan M, Shen T, Tang W, et al. Aging and aging-related diseases: from molecular mechanisms to interventions and treatments. *Signal Transduct Target Ther.* 2022 Dec 16;7(1):391.
7. UNHCR [Internet]. 2020 [cited 2023 Sep 29]. Older persons. Available from: <https://emergency.unhcr.org/protection/persons-risk/older-persons>
8. Fariñas DR. Un perfil de las personas mayores en España 2022. *Inf Envejec En Red [Internet].* 2022 Sep;(29). Available from: <https://envejecimientoenred.csic.es/>
9. Uotinen V. I'm as old as I feel. Subjective age in Finnish adults. *Univ Jyvask.* 2005;66.
10. Foo H, Mather KA, Thalamuthu A, Sachdev PS. The many ages of man: diverse approaches to assessing ageing-related biological and psychological measures and their relationship to chronological age. *Curr Opin Psychiatry.* 2019 Mar;32(2):130–7.
11. Maltoni R, Ravaioli S, Bronte G, Mazza M, Cerchione C, Massa I, et al. Chronological age or biological age: What drives the choice of adjuvant treatment in elderly breast cancer patients? *Transl Oncol.* 2022 Jan;15(1):101300.
12. Aguilera A, García-Muse T. Causes of genome instability. *Annu Rev Genet.* 2013;47:1–32.
13. Watts G. Leonard Hayflick and the limits of ageing. *The Lancet.* 2011 Jun

18;377(9783):2075.

14. Zhu Y, Liu X, Ding X, Wang F, Geng X. Telomere and its role in the aging pathways: telomere shortening, cell senescence and mitochondria dysfunction. *Biogerontology*. 2019 Feb;20(1):1–16.

15. Hipp MS, Park SH, Hartl FU. Proteostasis impairment in protein-misfolding and -aggregation diseases. *Trends Cell Biol*. 2014 Sep;24(9):506–14.

16. Dikic I, Elazar Z. Mechanism and medical implications of mammalian autophagy. *Nat Rev Mol Cell Biol*. 2018 Jun;19(6):349–64.

17. Fakouri NB, Hou Y, Demarest TG, Christiansen LS, Okur MN, Mohanty JG, et al. Toward understanding genomic instability, mitochondrial dysfunction and aging. *FEBS J*. 2019 Mar;286(6):1058–73.

18. Rhinn M, Ritschka B, Keyes WM. Cellular senescence in development, regeneration and disease. *Dev Camb Engl*. 2019 Oct 1;146(20):dev151837.

19. López-Otín C, Blasco MA, Partridge L, Serrano M, Kroemer G. The hallmarks of aging. *Cell*. 2013 Jun 6;153(6):1194–217.

20. Fafián-Labora JA, O’Loghlen A. Classical and Nonclassical Intercellular Communication in Senescence and Ageing. *Trends Cell Biol*. 2020 Aug;30(8):628–39.

21. Shannon OM, Ashor AW, Scialo F, Saretzki G, Martin-Ruiz C, Lara J, et al. Mediterranean diet and the hallmarks of ageing. *Eur J Clin Nutr*. 2021 Aug;75(8):1176–92.

22. Gude NA, Broughton KM, Firouzi F, Sussman MA. Cardiac ageing: extrinsic and intrinsic factors in cellular renewal and senescence. *Nat Rev Cardiol*. 2018 Sep;15(9):523–42.

23. Blaha MJ, DeFilippis AP. Multi-Ethnic Study of Atherosclerosis (MESA): JACC Focus Seminar 5/8. *J Am Coll Cardiol*. 2021 Jun 29;77(25):3195–216.

24. Puig J, Biarnes C, Pedraza S, Vilanova JC, Pamplona R, Fernández-Real JM, et al. The Aging Imageomics Study: rationale, design and baseline characteristics of the study population. *Mech Ageing Dev*. 2020 Jul;189:111257.

25. Schott JM. The neurology of ageing: what is normal? *Pract Neurol*. 2017 Jun;17(3):172–82.

26. Markov NT, Lindbergh CA, Staffaroni AM, Perez K, Stevens M, Nguyen K, et al.

Age-related brain atrophy is not a homogenous process: Different functional brain networks associate differentially with aging and blood factors. *Proc Natl Acad Sci*. 2022 Dec 6;119(49):e2207181119.

27. DeBette S, Markus HS. The clinical importance of white matter hyperintensities on brain magnetic resonance imaging: systematic review and meta-analysis. *BMJ*. 2010 Jul 26;341:c3666.

28. Sudre CH, Smith L, Atkinson D, Chaturvedi N, Ourselin S, Barkhof F, et al. Cardiovascular Risk Factors and White Matter Hyperintensities: Difference in Susceptibility in South Asians Compared With Europeans. *J Am Heart Assoc Cardiovasc Cerebrovasc Dis*. 2018 Oct 31;7(21):e010533.

29. Wu A, Sharrett AR, Gottesman RF, Power MC, Mosley TH, Jack CR, et al. Association of Brain Magnetic Resonance Imaging Signs With Cognitive Outcomes in Persons With Nonimpaired Cognition and Mild Cognitive Impairment. *JAMA Netw Open*. 2019 May 3;2(5):e193359.

30. Blinkouskaya Y, Weickenmeier J. Brain Shape Changes Associated With Cerebral Atrophy in Healthy Aging and Alzheimer's Disease. *Front Mech Eng [Internet]*. 2021 [cited 2023 Oct 9];7. Available from: <https://www.frontiersin.org/articles/10.3389/fmech.2021.705653>

31. Brickman AM, Honig LS, Scarmeas N, Tatarina O, Sanders L, Albert MS, et al. Measuring cerebral atrophy and white matter hyperintensity burden to predict the rate of cognitive decline in Alzheimer disease. *Arch Neurol*. 2008 Sep;65(9):1202–8.

32. Gur RC, Mozley PD, Resnick SM, Gottlieb GL, Kohn M, Zimmerman R, et al. Gender differences in age effect on brain atrophy measured by magnetic resonance imaging. *Proc Natl Acad Sci U S A*. 1991 Apr 1;88(7):2845–9.

33. Maillard P, Seshadri S, Beiser A, Himali JJ, Au R, Fletcher E, et al. Effects of systolic blood pressure on white-matter integrity in young adults in the Framingham Heart Study: a cross-sectional study. *Lancet Neurol*. 2012 Dec;11(12):1039–47.

34. Austin TR, Nasrallah IM, Erus G, Desiderio LM, Chen LY, Greenland P, et al. Association of Brain Volumes and White Matter Injury With Race, Ethnicity, and Cardiovascular Risk Factors: The Multi-Ethnic Study of Atherosclerosis. *J Am Heart Assoc*. 2022 Apr 5;11(7):e023159.

35. Scuteri A, Coluccia R, Castello L, Nevola E, Brancati AM, Volpe M. Left ventricular mass increase is associated with cognitive decline and dementia in the elderly independently of blood pressure. *Eur Heart J*. 2009 Jun;30(12):1525–9.
36. Elias MF, Sullivan LM, Elias PK, D’Agostino RB, Wolf PA, Seshadri S, et al. Left Ventricular Mass, Blood Pressure, and Lowered Cognitive Performance in the Framingham Offspring. *Hypertension*. 2007 Mar;49(3):439–45.
37. Defunciones según la Causa de Muerte. Instituto Nacional de Estadística [Internet]. 2023 Jun 27; Available from: https://www.ine.es/prensa/edcm_2022.pdf
38. Abdellatif M, Rainer PP, Sedej S, Kroemer G. Hallmarks of cardiovascular ageing. *Nat Rev Cardiol*. 2023 May 16;
39. Singam NSV, Fine C, Fleg JL. Cardiac changes associated with vascular aging. *Clin Cardiol*. 2020 Feb;43(2):92–8.
40. Diastole definition and meaning | Collins English Dictionary [Internet]. 2023 [cited 2023 Oct 2]. Available from: <https://www.collinsdictionary.com/dictionary/english/diastole>
41. Takeuchi M, Kitano T, Nabeshima Y, Otsuji Y, Otani K. Left ventricular and left atrial volume ratio assessed by three-dimensional echocardiography: Novel indices for evaluating age-related change in left heart chamber size. *Physiol Rep*. 2019;7(23):e14300.
42. Changes in cardiac structure and function with aging. *Complex Eng Syst*. 2022 Jan 12;2(1):13.
43. Steenman M, Lande G. Cardiac aging and heart disease in humans. *Biophys Rev*. 2017 Mar 20;9(2):131–7.
44. Fiechter M, Fuchs TA, Gebhard C, Stehli J, Klaeser B, Stähli BE, et al. Age-related normal structural and functional ventricular values in cardiac function assessed by magnetic resonance. *BMC Med Imaging*. 2013 Feb 7;13:6.
45. Cutrì E, Serrani M, Bagnoli P, Fumero R, Costantino ML. The cardiac torsion as a sensitive index of heart pathology: A model study. *J Mech Behav Biomed Mater*. 2015 Mar;55:104–19.
46. Rajiah PS, Kalisz K, Broncano J, Goerne H, Collins JD, François CJ, et al. Myocardial Strain Evaluation with Cardiovascular MRI: Physics, Principles, and Clinical Applications.

Radiogr Rev Publ Radiol Soc N Am Inc. 2022;42(4):968–90.

47. Olaya P, Sánchez J, Osio LF. Strain y strain rate para dummies. *Rev Colomb Cardiol*. 2011 Dec;18(6):340–4.
48. Qaja E, Tadi P, Theetha Kariyanna P. Carotid Artery Stenosis. In: StatPearls [Internet]. Treasure Island (FL): StatPearls Publishing; 2023 [cited 2023 Oct 13]. Available from: <http://www.ncbi.nlm.nih.gov/books/NBK442025/>
49. Hyperarts RM. Department of Surgery - Carotid Artery Disease [Internet]. [cited 2023 Oct 13]. Available from: <https://surgery.ucsf.edu/conditions--procedures/carotid-artery-disease.aspx>
50. Bamberg F, Kauczor HU, Weckbach S, Schlett CL, Forsting M, Ladd SC, et al. Whole-Body MR Imaging in the German National Cohort: Rationale, Design, and Technical Background. *Radiology*. 2015 Oct;277(1):206–20.
51. Berger A. Magnetic resonance imaging. *BMJ*. 2002 Jan 5;324(7328):35.
52. Hamet P, Tremblay J. Artificial intelligence in medicine. *Metabolism*. 2017 Apr 1;69:S36–40.
53. Martí R, Parramon D, García-Ortiz L, Rigo F, Gómez-Marcos MA, Sempere I, et al. Improving interMediAte risk management. MARK study. *BMC Cardiovasc Disord*. 2011 Oct 13;11:61.
54. Corominas Barnadas JM, López-Pousa S, Vilalta-Franch J, Calvó-Perxas L, Juvinyà Canal D, Garre-Olmo J. [MESGI50 study: description of a cohort on Maturity and Satisfactory Ageing]. *Gac Sanit*. 2017;31(6):511–7.
55. Mascarenhas NB, Muthupillai R, Cheong B, Pereyra M, Flamm SD. Fast 3D Cine Steady-State Free Precession Imaging with Sensitivity Encoding for Assessment of Left Ventricular Function in a Single Breath-Hold. *Am J Roentgenol*. 2006 Nov;187(5):1235–9.
56. Wetzel SG, Johnson G, Tan AGS, Cha S, Knopp EA, Lee VS, et al. Three-Dimensional, T1-Weighted Gradient-Echo Imaging of the Brain with a Volumetric Interpolated Examination. *AJNR Am J Neuroradiol*. 2002 Jun;23(6):995–1002.
57. King J, Lowery DR. Physiology, Cardiac Output. In: StatPearls [Internet]. Treasure Island (FL): StatPearls Publishing; 2023 [cited 2023 Oct 18]. Available from: <http://www.ncbi.nlm.nih.gov/books/NBK470455/>

58. Sierra C. [Hypertension in older adults]. *Hipertens Riesgo Vasc.* 2017;34 Suppl 2:26–9.
59. Left Ventricular Hypertrophy - StatPearls - NCBI Bookshelf [Internet]. [cited 2023 Oct 24]. Available from: <https://www.ncbi.nlm.nih.gov/books/NBK557534/>
60. Kahan T, Bergfeldt L. Left ventricular hypertrophy in hypertension: its arrhythmogenic potential. *Heart.* 2005 Feb 1;91(2):250–6.

13. ANNEXES

13.1. ANNEX 1 – ETHICS COMMITTEE PROJECT APPROVAL



Avinguda de França s/n.
17007 Girona
Telèfon 972 940 200
www.gencat.net/ics/trueta


Marta Riera Juncà, Secretària del Comitè d'Ètica d'Investigació CEI GIRONA, amb domicili a l'Hospital Universitari de Girona Dr. Josep Trueta Avinguda de França s/n 17007 Girona

CERTIFICA

Que el Comitè d'Ètica d'Investigació CEI GIRONA, segons consta en l'acta de la reunió celebrada el dia 24/10/2017 ha avaluat el projecte: **Imagenoma de l'envelliment: Estudi observacional poblacional per al desenvolupament de biomarcadors d'imatge corporal integral basats en ressonància magnètica en individus de 50 anys d'edat o més i la seva relació amb factors de l'esfera biopsicosocial, cardiovascular, metabòlica, lipídica, microbiòmica i altres factors associats a l'envelliment. Cod SLT002-16/00250.** Protocol v. 01:01/09/17 QRD v01:01/09/17, FIP i CI v2:28/09/17 i FIP i CI obtenció mostra directe Biobanc col IME v1:set 17 v en català i castellà, FIP i CI projecte amb final Biobanc col IME v1:set 17 v en català i castellà amb el Dr. JOSEP PUIG ALCÁNTARA com a investigador principal.

Que els documents s'ajusten a les normes ètiques essencials i per tant, ha decidit la seva aprovació.

I, perquè consti, expedeixo aquest certificat.


Hospital Universitari de Girona
Doctor Josep Trueta
Comitè Ètic
d'Investigació Clínica
Institut Català de la Salut

Girona, a 27 d'octubre de 2017

13.2. ANNEX 2 – INFORMATION SHEET FOR PARTICIPANTS

FULL D'INFORMACIÓ AL PARTICIPANT DE L'ESTUDI "IMAGENOMA DE L'ENVELLIMENT"

Benvolguda/Benvolgut,

Agraïm novament la seva col·laboració en l'estudi MESGI50 (Maduresa i Envelliment Satisfactori a Girona) que realitzem a diversos municipis de les comarques gironines i en el qual vostè hi participa des de l'any 2013. Aquest estudi està contribuint a millorar els coneixements que tenim sobre quines són i com canvien les circumstàncies vitals de les persones a partir dels 50 anys.

Els investigadors d'aquest estudi estem molt interessants en conèixer l'estat de salut dels participants i l'efecte que diverses malalties poden provocar durant el procés d'envelliment i en la qualitat de vida de les persones. Per aquest motiu s'ha constituït un grup de recerca que incorpora investigadors de l'Institut d'Investigació Biomèdica de Girona, de l'Institut de Recerca Biomèdica de Lleida, de l'Hospital Universitari Dr. Josep Trueta de Girona, de l'Institut d'Assistència Sanitària, de la Universitat de Girona i de la Universitat Pompeu Fabra de Barcelona per fer un MESGI50 encara més complet que incorpori diverses proves mèdiques, el **+MESGI50** i hem dissenyat un projecte de recerca que s'anomena **IMAGENOMA DE L'ENVELLIMENT**. El grup està compost per 44 investigadors de diferents especialitat com la imatge mèdica, la cardiologia, la endocrinologia, la neurologia, l'atenció primària, la microbiologia, la neuropsicologia, la bioestadística i la nutrició entre d'altres.

Abans que decideixi si participa en aquest estudi o no, és important que conegui quins són els objectius de l'estudi i què implica la seva participació. Si us plau, faci servir el temps que necessiti per a llegir tota la informació amb deteniment abans de prendre una decisió.

Quina és la finalitat de l'estudi?

L'estudi IMAGENOMA DE L'ENVELLIMENT vol desenvolupar marcadors d'imatge corporal basats en ressonància magnètica (que és una prova mèdica que utilitza un potent imant i ones de ràdio per poder visualitzar amb detall estructures internes del nostre cos) i conèixer la relació que hi ha amb altres marcadors de salut, com per exemple, els resultats d'una analítica de sang, el resultat d'un electrocardiograma o la seva capacitat de memòria entre molts altres marcadors de salut.

Per què és important aquest estudi?

Els resultats d'aquest estudi poden ajudar a conèixer millor el procés d'envelliment biològic del nostre cos i la seva relació amb moltes malalties freqüents en aquesta etapa de la vida com la hipertensió arterial, la diabetis o la malaltia d'Alzheimer entre d'altres. En la mesura en que l'estudi analitzarà molta informació sobre l'estil de vida i la salut això permetrà poder identificar factors de risc i desenvolupar recomanacions per promoure un procés d'envelliment satisfactori.

Per què em conviden a participar?

El convidem a participar perquè vostè ja forma part d'un estudi sobre la Maduresa i l'Envelliment Satisfactori a Girona, l'estudi MESGI i en l'entrevista que hem fet aquest any en el seu domicili ens va expressar el seu interès en participar.

Haig de participar obligatòriament?

No, en absolut. La seva participació és totalment voluntària i en qualsevol moment pot deixar de participar en l'estudi sense haver d'explicar-ne els motius.

En què consistirà la meva participació?

Si decideix participar se li programaran dues visites al Parc Hospitalari Martí i Julià de Salt on es troben les instal·lacions i aparells necessaris per fer les proves d'aquest estudi. En la **primera visita** se li farà la ressonància magnètica de cos sencer, una ecografia de les arteries del coll i un estudi de la composició corporal. Al finalitzar aquestes proves se li informarà sobre el procediment de recollida de mostres biològiques de la segona visita,

se li facilitarà un pot per recollir una mostra de femta, un pot per recollir una mostra d'orina i uns senzills qüestionaris que s'hauran d'entregar a la segona visita. A la **segona visita** haurà de venir en dejú per tal de fer una extracció sanguínia i haurà d'entregar el pot amb la mostra de femta i el pot amb la mostra d'orina per tal de cedir i formalitzar la donació de les mostres al Biobanc de l'Institut d'Investigació Biomèdica de Girona per futures investigacions. Previ a l'entrada de la mostra de sang al Biobanc, es farà una determinació dels paràmetres bioquímics més freqüents. També haurà d'entregar els qüestionaris de la primera visita. A continuació se li realitzarà un electrocardiograma, una exploració física que inclourà mesures de pressió i rigidesa arterial i un conjunt de proves per avaluar el seu estat d'ànim i diferents funcions mentals com la memòria, l'atenció o la capacitat visual i perceptiva.

Com s'utilitzaran les meves dades en aquest estudi?

Participant en aquest estudi realitzaria una contribució de gran valor per a la investigació científica. Les dades obtingudes de tots els participants només s'utilitzaran per a fins d'investigació científica. A la llarga, els resultats seran publicats en revistes científiques i presentats en congressos científics. Evidentment, les publicacions i presentacions mai contindran el nom o una altra informació que permeti identificar les persones que hi ha participat. L'ús comercial d'aquestes dades està estrictament prohibit i no es vendran mai ni les mostres ni els resultats.

A la base de dades del projecte IMAGENOMA DE L'ENVELLIMENT no hi apareixerà ni el nom ni cap altre dada de caràcter personal que el pugui identificar. Les dades que es registrin seran codificades en una base de dades que mantindrà la confidencialitat de la informació de tots els participants. A cada registre individual se li assignarà un codi, de manera que no serà possible conèixer la identitat de cap dels participants.

Totes les dades que generi aquest estudi seran estrictament confidencials i només hi tindran accés els investigadors, les autoritat sanitàries, els membres del Comitè Ètic d'Investigació Clínica i el personal autoritzat per garantir la qualitat i l'anàlisi de les dades, tal com obliga la Llei Orgànica 15/1999 de 13 de desembre, de Protecció de dades de

caràcter personal. Totes les dades seran processades, analitzades i guardades a l'Institut d'Investigació Biomèdica de Girona amb domicili a Carrer del Dr. Castany, s/n, 17190 de Salt i a l'Institut de Recerca Biomèdica de Lleida amb domicili a Av. Alcalde Rovira Roure, 80, 25198 de Lleida. Les mostres de sang, femta i orina recollides seran processades i custodiades al Biobanc IDIBGi per futures investigacions. Vostè podrà exercir en qualsevol moment els seus drets d'accés, rectificació, cancel·lació i oposició, així com obtenir informació sobre l'ús de les seves mostres i dades associades, dirigint-se a:

Dr. Josep Puig
Institut de Diagnòstic per la Imatge.
Institut d'Investigació Biomèdica de Girona.
Hospital Universitari Dr. Josep Trueta de Girona. Av de França s/n; 17007 Girona
Tel: 972 486 020 / Fax: 972 486 085

Quins riscos i beneficis tindrà si participo?

La ressonància magnètica no representa cap risc per a la seva salut. Tanmateix, si vostè porta un marcapassos, implants a l'oïda interna (coclears), articulacions artificials recentment implantades o algun tipus especial de vàlvula cardíaca no podrà fer-se la prova. Abans de fer la ressonància magnètica els investigadors li faran un seguit de preguntes per garantir la seva seguretat en la realització de la ressonància magnètica. Els riscos associats a la punxada per a la realització de l'extracció de sang són els mateixos que els que podria experimentar per una analítica sol·licitada pel seu metge de família. En general, l'extracció de sang s'associa a riscos petits, encara que podria causar una mica de dolor, un petit hematoma per on entra l'agulla o ansietat davant les agulles. Les inflamacions o la lesió dels nervis o del sistema vascular només succeeixen en casos extremadament rars. Es prendran precaucions per a evitar aquests inconvenients per part dels professionals sanitaris de l'estudi. La recollida de la mostra de femta i orina no suposarà cap risc afegit per a vostè.

Un benefici important pel fet de participar en aquest estudi és que a vostè se li farà una extensa bateria de proves mèdiques i en el cas que es detecti alguna anomalia que

requereixi una atenció mèdica específica vostè serà informat i derivat als dispositius sanitaris oportuns (metge especialista en medicina familiar i comunitària o metge especialista hospitalari). En el cas de que no volgués ser informat dels resultats de les proves mèdiques haurà d'especificar-ho en el full de sol·licitud de rebuig a ser informat dels resultats de les exploracions mèdiques.

Quines avantatges i inconvenients tindrà si participo?

Si decideix participar en l'estudi se li proporcionarà un informe complet amb els resultats de la prova de ressonància magnètica on es detallarà l'estat de diferents parts del seu cos com el cervell, el cor, el fetge, la arteria aorta, la columna vertebral i les articulacions. També se li farà arribar al seu domicili els resultats de l'analítica de sang i l'electrocardiograma perquè vostè ho pugui compartir amb el seu metge de família si ho considera convenient. Així mateix, d'acord amb els resultats obtinguts, rebrà un conjunt de recomanacions per afavorir el seu estat de salut. Tots els resultats de les proves mèdiques li facin no tindran cap cost econòmic per a vostè, però tampoc rebrà cap compensació econòmica per la seva participació.

El principal inconvenient de participar en aquest estudi és que haurà de desplaçar-se en dues ocasions al Parc Hospitalari Martí i Julià de Salt per tal que els tècnics i professionals de l'estudi hi facin les proves, recullin les mostres biològiques i li facin un conjunt de preguntes i tests per conèixer el seu estat de salut. La durada prevista de cada visita és de una hora i l'interval entre la primera i segona visita serà de uns 15 dies aproximadament (els gestors del l'estudi s'ajustaran a la seva disponibilitat per programar les visites). La primera visita la podrà fer o bé al matí o bé a la tarda. Tanmateix, la segona visita es farà pel matí, vostè haurà de venir en dejú per tal de fer l'extracció de sang i proporcionar una mostra de femta en el pot especial que se li proporcionarà en la primera visita. Està previst també habilitar alguns caps de setmana per facilitar les visites de les persones que per compromisos laborals o familiars tinguin dificultats per desplaçar-se entre setmana.

Qui ha revisat aquest estudi?

Aquest document ha estat revisat i aprovat pel Comitè Ètic d'Investigació Clínica de l'Hospital Universitari Dr. Josep Trueta. Aquest comitè té la responsabilitat de garantir que els estudis acompleixin les normes vigents i els protocols de bona pràctica clínica i ètica.

Qui finança aquest estudi?

Aquest estudi està finançat per una beca competitiva del Pla Estratègic de Recerca i Innovació en Salut (2016-2020) del Departament de Salut de la Generalitat de Catalunya amb l'objectiu de generar nou coneixement que tingui una repercussió directa en la millora de la salut dels ciutadans.

A qui puc dirigir-me per demanar més informació?

Per a més informació, pot posar-se en contacte amb l'investigador principal de l'estudi MESGI50 o bé amb l'investigador principal del projecte IMAGENOMA DE L'ENVELLIMENT. No dubti a consultar-l'hi si ho considera necessari. Si us plau, pregunti tots els dubtes que tingui i prengui's el temps necessari per decidir si vol participar en aquest estudi.

Dr. Josep Puig. Institut de Diagnòstic per la Imatge Institut d'Investigació Biomèdica de Girona Hospital Universitari Dr. Josep Trueta de Girona Av de França s/n; 17007 Girona Tel: 972 486 020 / Fax: 972 486 085	Dr. Josep Garre-Olmo Institut d'Assistència Sanitària Institut d'Investigació Biomèdica de Girona Edifici Mancomunitat 1 C/ Dr Castany s/n 17190 Salt Tel: 972 182 600 / Fax: 972 486 085
---	--

Una vegada més, li agraïm molt l'atenció que ens ha dispensat.

13.3. ANNEX 3 – INFORMED CONSENT

FORMULARI DE CONSENTIMENT INFORMAT AL PARTICIPANT DE L'ESTUDI "IMAGENOMA DE L'ENVELLIMENT"

Jo, _____
(Nom i cognoms)

He llegit el full d'informació que m'han lliurat.

He pogut fer preguntes sobre l'estudi 'IMAGENOMA DE L'ENVELLIMENT'.

He rebut suficient informació sobre l'estudi.

He parlat amb Josep Puig o col·laborador, amb telèfon de contacte 972486020 i declaro que

- Comprenc que la meva participació és voluntària
- Comprenc que puc retirar-me de l'estudi quan vulgui sense haver de donar explicacions
- Presto lliurement la meva conformitat per participar en l'estudi

Consento expressament a participar en l'estudi i entenc que amb la meva participació

Consento expressament en el tractament de les meves dades personals i de salut.

I manifesto que les dades facilitades per l'estudi són exactes i veraces.

A _____ (lloc) , a _____ (dia) de _____ (mes) de
_____ (any)

Data _____ Firma del participant _____

Data _____ Nom i firma de l'informador _____

13.4. ANNEX 4 – REFUSE TO BE INFORMED OF INCIDENTAL FINDINGS

REBUIG A SER INFORMAT DELS RESULTATS DE L'EXPLORACIÓ DE RM REALITZADA DE L'ESTUDI "IMAGENOMA DE L'ENVELLIMENT"

Jo, _____
(Nom i cognoms)

He llegit el full d'informació que se m'ha lliurat i he signat el consentiment a participar en l'estudi.

He rebut suficient informació sobre l'estudi i he pogut fer preguntes sobre l'estudi.

Consento expressament a participar en l'estudi i entenc que amb la meva participació.

Consento expressament el tractament de les meves dades personals i de salut.

Declaro que;

Tot i la meva participació en l'estudi NO vull ser informat dels resultats obtinguts en l'exploració de ressonància magnètica realitzada.

A _____ (lloc) , a _____ (dia) de _____ (mes) de _____ (any)

Data _____ Firma del participant _____

Data _____ Nom i Firma de l'informador _____

13.5. ANNEX 5 – ANALYSIS ADJUSTED FOR AGE

ANNEX 5: Multivariate results adjusted for age.					
Variables	WMH	Cortex volume	Cortex volume without ventricles	Cortical white matter volume	Total grey matter volume
LV end-diastolic mass ^{BS} , mean (SD)	0.05 (0.03,0.08) [p<0.001]*	0.50 (0.21,0.78) [p<0.001]*	1.25 (0.45,2.05) [0.002]*	0.61 (0.12,1.10) [0.015]*	0.64 (0.29,0.99) [p<0.001]*
LV end-diastolic volume ^{BS} , mean (SD)	0.02 (0.00,0.03) [0.012]*	0.26 (0.09,0.43) [0.003]*	0.64 (0.15,1.13) [0.010]*	0.33 (0.03,0.63) [0.029]*	0.32 (0.11,0.53) [0.003]*
LV end-systolic volume ^{BS} , mean (SD)	0.02 (- 0.00,0.04) [0.116]	0.32 (0.06,0.59) [0.018]*	0.80 (0.04,1.56) [0.039]*	0.43 (- 0.03,0.89) [0.068]	0.38 (0.05,0.71) [0.025]*
LV mass/volume index ^{BS} , mean (SD)	1.00 (- 0.46,2.47) [0.180]	1.26 (- 15.94,18.46) [0.886]	8.32 (- 40.59,57.23) [0.738]	3.18 (- 26.57,32.93) [0.834]	3.91 (- 17.37,25.19) [0.718]
LV ejection fraction, mean (SD)	-0.00 (- 0.03,0.02) [0.846]	-0.16 (- 0.44,0.12) [0.267]	-0.44 (- 1.24,0.36) [0.283]	-0.24 (- 0.72,0.25) [0.339]	-0.20 (- 0.55,0.15) [0.258]
LV stroke volume ^{BS} , mean (SD)	0.03 (0.01,0.05) [0.015]*	0.33 (0.05,0.61) [0.020]*	0.80 (0.02,1.59) [0.046]*	0.40 (- 0.08,0.88) [0.105]	0.42 (0.07,0.76) [0.017]*
LV cardiac output ^{BS} , mean (SD)	0.37 (0.03,0.72) [0.034]*	4.18 (0.14,8.23) [0.043]*	10.05 (- 1.46,21.57) [0.087]	4.80 (- 2.21,11.81) [0.179]	5.37 (0.36,10.37) [0.036]*
LV Global longitudinal strain, mean (SD)	0.04 (- 0.01,0.09) [0.104]	0.20 (- 0.35,0.75) [0.472]	0.90 (- 0.65,2.45) [0.255]	0.40 (- 0.53,1.34) [0.398]	0.47 (- 0.22,1.15) [0.180]
LV Global circumferential strain, mean (SD)	0.02 (- 0.01,0.04) [0.155]	0.16 (- 0.13,0.45) [0.275]	0.50 (- 0.32,1.31) [0.232]	0.20 (- 0.29,0.70) [0.419]	0.27 (- 0.09,0.63) [0.136]
LV Global radial strain, mean (SD)	0.00 (- 0.00,0.01) [0.238]	0.00 (- 0.06,0.06) [0.981]	0.08 (- 0.10,0.26) [0.382]	0.06 (- 0.05,0.17) [0.280]	0.02 (- 0.06,0.09) [0.695]
RV end-diastolic volume ^{BS} , mean (SD)	0.01 (- 0.00,0.02) [0.156]	0.51 (0.35,0.67) [p<0.001]*	1.30 (0.83,1.76) [p<0.001]*	0.62 (0.34,0.90) [p<0.001]*	0.67 (0.47,0.87) [p<0.001]*
RV end-systolic volume ^{BS} , mean (SD)	0.01 (- 0.01,0.04) [0.384]	1.05 (0.77,1.33) [p<0.001]*	2.87 (2.07,3.67) [p<0.001]*	1.50 (1.01,1.99) [p<0.001]*	1.32 (0.97,1.66) [p<0.001]*
RV ejection fraction, mean (SD)	0.00 (- 0.02,0.02) [0.917]	-0.49 (-0.74,- 0.25) [p<0.001]*	-1.54 (-2.24,- 0.83) [p<0.001]*	-0.92 (-1.35,- 0.49) [p<0.001]*	-0.57 (-0.88,- 0.26) [p<0.001]*
RV stroke volume ^{BS} , mean (SD)	0.01 (- 0.01,0.03) [0.188]	0.34 (0.11,0.58) [0.005]*	0.74 (0.07,1.41) [0.031]*	0.27 (- 0.14,0.68) [0.203]	0.48 (0.19,0.78) [0.001]*

The coefficients marked with an asterisk (*) are statistically significant results. Variables marked with a BS superscript have been normalized by body surface (BS) area. Abbreviations: WMH: White matter hyperintensities, LV: Left ventricle, RV: Right ventricle, SD: Standard deviation.

13.6. ANNEX 6 – ANALYSIS ADJUSTED FOR DEGREE OF STENOSIS

ANNEX 6: Multivariate results adjusted for the degree of carotid stenosis.					
Variables	WMH	Cortex volume	Cortex volume without ventricles	Cortical white matter volume	Total grey matter volume
LV end-diastolic mass ^{BS} , mean (SD)	0.05 (0.02,0.07) [p<0.001]*	0.52 (0.22,0.81) [p<0.001]*	1.25 (0.41,2.09) [0.003]*	0.61 (0.11,1.12) [0.018]*	0.64 (0.28,1.01) [p<0.001]*
LV end-diastolic volume ^{BS} , mean (SD)	0.01 (-0.00,0.03) [0.157]	0.32 (0.15,0.50) [p<0.001]*	0.81 (0.31,1.31) [0.002]*	0.42 (0.11,0.72) [0.007]*	0.39 (0.17,0.61) [p<0.001]*
LV end-systolic volume ^{BS} , mean (SD)	0.01 (-0.01,0.03) [0.405]	0.38 (0.11,0.66) [0.007]*	0.96 (0.17,1.74) [0.017]*	0.51 (0.04,0.98) [0.035]*	0.45 (0.11,0.79) [0.010]*
LV mass/volume index ^{BS} , mean (SD)	1.65 (0.14,3.17) [0.032]*	-7.01 (-24.71,10.69) [0.437]	-17.89 (-68.25,32.46) [0.486]	-10.25 (-40.56,20.06) [0.507]	-8.11 (-30.13,13.91) [0.470]
LV ejection fraction, mean (SD)	0.00 (-0.02,0.03) [0.927]	-0.18 (-0.48,0.11) [0.212]	-0.51 (-1.33,0.32) [0.229]	-0.27 (-0.77,0.23) [0.283]	-0.23 (-0.59,0.13) [0.208]
LV stroke volume ^{BS} , mean (SD)	0.02 (-0.01,0.04) [0.157]	0.42 (0.14,0.71) [0.003]*	1.08 (0.26,1.89) [0.009]*	0.54 (0.05,1.02) [0.032]*	0.54 (0.19,0.89) [0.003]*
LV cardiac output ^{BS} , mean (SD)	0.21 (-0.14,0.57) [0.242]	5.48 (1.31,9.65) [0.010]*	13.65 (1.78,25.51) [0.024]*	6.62 (-0.53,13.77) [0.069]	7.02 (1.84,12.20) [0.008]*
LV Global longitudinal strain, mean (SD)	0.04 (-0.01,0.09) [0.095]	0.16 (-0.41,0.72) [0.589]	0.74 (-0.86,2.34) [0.365]	0.32 (-0.63,1.28) [0.508]	0.39 (-0.32,1.09) [0.280]
LV Global circumferential strain, mean (SD)	0.02 (-0.01,0.05) [0.113]	0.14 (-0.16,0.43) [0.359]	0.42 (-0.42,1.26) [0.330]	0.16 (-0.34,0.67) [0.532]	0.24 (-0.13,0.61) [0.203]
LV Global radial strain, mean (SD)	0.00 (-0.00,0.01) [0.479]	0.01 (-0.05,0.08) [0.743]	0.11 (-0.08,0.29) [0.254]	0.07 (-0.04,0.19) [0.193]	0.03 (-0.05,0.11) [0.491]
RV end-diastolic volume ^{BS} , mean (SD)	0.00 (-0.01,0.02) [0.676]	0.57 (0.40,0.73) [p<0.001]*	1.46 (0.99,1.94) [p<0.001]*	0.71 (0.42,0.99) [p<0.001]*	0.74 (0.53,0.95) [p<0.001]*
RV end-systolic volume ^{BS} , mean (SD)	0.00 (-0.02,0.03) [0.759]	1.10 (0.81,1.39) [p<0.001]*	3.01 (2.19,3.84) [p<0.001]*	1.58 (1.07,2.08) [p<0.001]*	1.38 (1.02,1.74) [p<0.001]*
RV ejection fraction, mean (SD)	-0.00 (-0.02,0.02) [0.819]	-0.45 (-0.70,-0.19) [p<0.001]*	-1.38 (-2.11,-0.65) [p<0.001]*	-0.84 (-1.29,-0.40) [p<0.001]*	-0.50 (-0.82,-0.18) [0.002]*
RV stroke volume ^{BS} , mean (SD)	0.00 (-0.02,0.02) [0.728]	0.43 (0.19,0.67) [p<0.001]*	1.00 (0.31,1.69) [0.005]*	0.40 (-0.02,0.82) [0.062]	0.60 (0.30,0.90) [p<0.001]*

The coefficients marked with an asterisk (*) are statistically significant results. Variables marked with a BS superscript have been normalized by body surface (BS) area. Abbreviations: WMH: White matter hyperintensities, LV: Left ventricle, RV: Right ventricle, SD: Standard deviation.